

<https://helda.helsinki.fi>

Effects of added humic substances and nutrients on
photochemical degradation of dissolved organic matter in a
mesocosm amendment experiment in the Gulf of Finland, Baltic Sea

Ma, Kun

2022-09

Ma , K , Powers , L C , Seppälä , J , Norkko , J & Brandes , J A 2022 , ' Effects of added humic substances and nutrients on photochemical degradation of dissolved organic matter in a mesocosm amendment experiment in the Gulf of Finland, Baltic Sea ' , Photochemistry and Photobiology , vol. 98 , no. 5 , pp. 1025-1042 . <https://doi.org/10.1111/php.13597>

<http://hdl.handle.net/10138/353836>

<https://doi.org/10.1111/php.13597>

unspecified

acceptedVersion

Downloaded from Helda, University of Helsinki institutional repository.

This is an electronic reprint of the original article.

This reprint may differ from the original in pagination and typographic detail.

Please cite the original version.

MS. KUN MA (Orcid ID : 0000-0002-8532-8149)

Article type : Research Article

Effects of Added Humic Substances and Nutrients on Photochemical Degradation of Dissolved Organic Matter in A Mesocosm Amendment Experiment in the Gulf of Finland, Baltic Sea

Kun Ma¹, Leanne C. Powers^{1,2}, Jukka Seppälä³, Joanna Norkko⁴, Jay A. Brandes^{1*}

¹Skidaway Institute of Oceanography, Department of Marine Sciences, University of Georgia,
Savannah, GA, USA

²Department of Chemistry, State University of New York, College of Environmental Science and
Forestry, Syracuse, NY, USA

³Finnish Environment Institute, Marine Research Centre, Helsinki, Finland

⁴Tvärminne Zoological Station, University of Helsinki, Hanko, Finland

*Corresponding author e-mail: Jay.Brandes@skio.uga.edu (Jay A. Brandes)

This article has been accepted for publication and undergone full peer review but has not been through the copyediting, typesetting, pagination and proofreading process, which may lead to differences between this version and the [Version of Record](#). Please cite this article as [doi: 10.1111/PHP.13597](https://doi.org/10.1111/PHP.13597)

This article is protected by copyright. All rights reserved

ABSTRACT

Humic substances, a component of terrestrial dissolved organic matter (tDOM), contribute to dissolved organic matter (DOM) and chromophoric DOM (CDOM) in coastal waters, and have significant impacts on biogeochemistry. There are concerns in recent years over browning effects in surface waters, due to increasing tDOM inputs, and their negative impacts on aquatic ecosystems, but relatively little work has been published on estuaries and coastal waters. Photodegradation could be a significant sink for tDOM in coastal environments, but the rates and efficiencies are poorly constrained. We conducted large-scale DOM photodegradation experiments in mesocosms amended with humic substances and nutrients in the Gulf of Finland to investigate the potential of photochemistry to remove added tDOM and the interactions of DOM photochemistry with eutrophication. The added tDOM was photodegraded rapidly, as CDOM absorption decreased and spectral slopes increased with increasing photons absorbed in laboratory experiments. The *in situ* DOM optical properties became similar amongst the control, humic-, and humic+nutrients-amended mesocosm samples towards the end of the amendment experiment, indicating degradation of the excess CDOM/DOM through processes including photodegradation. Nutrient additions didn't significantly influence the effects of added humic substances on CDOM optical property changes, but induced changes in DOM removal.

INTRODUCTION

Dissolved organic matter (DOM) is the second largest bioreactive reservoir of carbon in the ocean after dissolved inorganic carbon (1-4), and plays an important role in many oceanographic processes such as supporting microbial growth (5-7). Marine DOM can be autochthonous or allochthonous, and one of the main allochthonous DOM sources is rivers (8), which supply from 0.17 Pg C y⁻¹ (9) to 0.36 Pg C y⁻¹ (10) of terrestrial DOM (tDOM) to the ocean. Humic substances, such as lignin polyphenols, are a component of tDOM (11) and can have significant impacts on the biogeochemistry of coastal waters (12). In coastal areas, soil humic substances can make a large contribution to the colored portion of the DOM pool (chromophoric dissolved organic matter, or CDOM), which has been attributed to their relatively high aromatic content (11). The ultimate fate of this material is still poorly understood and highly debated however, and we need a better understanding of how tDOM degrades in coastal systems.

In recent years, there are increasing concerns that climate change and anthropogenic activities can lead to increased terrestrial input of humic substances to surface waters and browning of surface waters, or browning effects (13, 14). Such effects, in turn, can affect carbon cycling and climate (15) and significantly impact aquatic ecosystems (16-22). Most studies on browning effects are on rivers and lakes, with relatively less work published on estuaries and coastal water environments at the receiving end of river supplied tDOM (23, 24). In addition, increased tDOM could have complex effects on coastal eutrophication processes depending on initial nutrients and tDOM conditions of the system (23, 24). For example, Andersson et al. (2013) conducted a mesocosm experiment using northern Baltic Sea water amended with humic carbon and inorganic nutrients to investigate the biological effects of browning from allochthonous DOM and the interaction of added humic carbon with nutrients, and found that the addition of humic carbon may counteract the effect of eutrophication (24).

Lauerwald et al. (25) estimated that at least 25 % of tDOM is removed before reaching the coast. The remaining tDOM fractions could be transformed in estuaries or coastal oceans (11, 26, 27, 23), through biotic (28-32) and abiotic processes such as flocculation (33, 34), sorption (35) and photodegradation (36-39, 31, 40, 32).

Photodegradation can lead to loss of color due to degradation of CDOM and subsequent decrease in CDOM absorbance (41, 42, 11). CDOM can also act as a photosensitizer, passing absorbed solar energy along and triggering a suite of secondary reactions that lead to the degradation of other DOM components (11). In coastal oceans and estuaries, especially for water with high tDOM input, color bleaching of water samples can often be a good indicator of DOM photolability (42).

Photodegradation of CDOM can have multiple effects on the local ecosystems, by changing the light availability, e.g., the penetration of photosynthetically active radiation and potentially harmful ultraviolet (UV) radiation (11, 43). Photodegradation of DOM can also lead to changes in biolability of DOM, for example, transformation of biologically recalcitrant DOM into biolabile substrates that supports bacterial growth (44). In addition, DOM photodegradation could influence the ocean-atmosphere fluxes of important atmospheric gases such as CO₂ through dissolved inorganic carbon (DIC) photoproduction (42). However, rates of CDOM and DOM photodegradation in coastal zones span a large range and the role of photochemistry in tDOM cycling is still poorly understood (45-47). Therefore, due to the presumed role of photochemistry in tDOM cycling/removal and considering potential future coastal water browning, more quantitative information on CDOM photobleaching and DOM photodegradation in coastal waters is sorely needed.

In the Baltic Sea, allochthonous tDOM contribute to a large portion (~43 - 83 %) of the high molecular weight DOM pool in the surface water (48), and photochemistry is thought to be a major sink for DOM, with the total photochemical transformation of dissolved organic carbon (DOC) (2.71 - 3.94 Tg C y⁻¹) exceeding the annual riverine input of allochthonous photoreactive DOC to the Baltic Sea (< 2.45 Tg C y⁻¹) (44). As large numbers of Finland lakes and streams are currently experiencing DOM concentration increases, or browning (14), it is conceivable that the Baltic Sea - at the receiving end of these freshwater systems - may in the future experience similar browning effects. In addition, coastal eutrophication is a prevailing problem in large portions of the Baltic Sea (49, 50). However, the potential of photochemistry to remove additional inputs of tDOM in the Gulf of Finland, as well as the interactions of DOM photochemistry with eutrophication, is not well constrained. It is expected that bacterial consumption and photodegradation of the added DOM could lead to a decrease in DOM and CDOM contents, but primary production may also add autochthonous DOM and/or CDOM to the system. A previous browning experiment at the IGB LakeLab in Germany indicated an interesting

and complex pattern of DOM composition change over the course of the experiment, suggesting that there are both losses and inputs of DOM to the mesocosms after amendments (Stella Berger, personal communication). To that end, we conducted large-scale DOM photodegradation experiments in mesocosms with and without added humic substances (to simulate coastal browning). Mesocosm experiments bridge small scale laboratory experiments and large scale environmental sampling, and are frequently conducted to assess the response of a system to changing conditions, such as added carbon or nutrients (23, 24). The LightCycle experiment was conducted to continue the investigation to constrain the photochemical sink of added humic substances to an estuarine system. We took mesocosm samples to monitor the changes occurred *in situ* after the addition of humic substances and nutrients, and conducted laboratory photoirradiation experiments using sterile-filtered mesocosm samples to examine only the effects of photodegradation. More specifically, the following hypotheses were tested in this study: 1) added humic substances can be photochemically degraded rapidly in this coastal Baltic Sea system, 2) comparing *in situ* and laboratory rates will reveal the importance of photodegradation in removing added humic substances, and 3) added nutrients will affect photochemical degradation of added humic substances.

MATERIALS AND METHODS

The AQUACOSM JOMEX experiments were mesocosm experiments covering a range of aquatic systems, and the JOMEX: Systems Responses to A Pulse of Dissolved Organic Carbon project, was one such experiment conducted at the Tvärminne Mesocosm Facility (TMF, Tvärminne Zoological Station (TZS), University of Helsinki, <https://www.aquacosm.eu/mesocosm/tvarminne-mesocosm-facility-tmf/>) in the Western Gulf of Finland. This Baltic Sea site is a brackish water estuarine environment (51, 52) and the experiment investigated the biological and physico-chemical system responses of this site to added humic substances and/or nutrients. The LightCycle experiment was a component of the JOMEX project, testing the photodegradation rates and trends of the added humic substances and native CDOM/DOM, as well as the interactions of DOM photochemistry with added inorganic nutrients (phosphate and ammonium).

Sampling: The JOMEX experiment ran from 26 June to 10 July 2019. The experimental setup consisted of 9 2000-L capacity (0.9 m diameter × 3 m depth) mesocosms at the TMF at 59.843144 N, 23.260337 E. Humic substances (Humintech GmbH HuminFeed® WSG) and nutrients (NH₄Cl and KH₂PO₄) were added to mesocosms on 26 June 2019 (day 1). The mesocosms were divided into three treatment groups: 3 control mesocosms with no humic substances or nutrients added, 3 humic-amended mesocosms with only humic substances added to a final concentration of 2 mg L⁻¹ in each mesocosm, and 3 humic+nutrients-amended mesocosms with humic substances (2 mg L⁻¹ final concentration) and NH₄Cl and KH₂PO₄ (80 μg L⁻¹ N and 20 μg L⁻¹ P final concentrations) added. All mesocosms were covered with transparent acrylic covers (cut off wavelength below ~380 nm) during the experiment.

The surface salinity at the mesocosm site was relatively low (5.6 - 6.1 for the 13 day sampling period of the LightCycle experiments) with little variation (5.8 ± 0.2). The surface water temperature was 15 °C at the beginning of the amendment experiment, but decreased to 11 °C on day 8 and stayed low, until it was one degree higher on day 13 at 12 °C.

Surface (1 m) water samples for our LightCycle experiments were collected using precleaned 10-L HDPE canisters (Plastex®, Finland) from one each of control, humic-amended and humic+nutrients-amended mesocosms, immediately after the amendment (day 1), and 2, 5, 7, 9, and 12 days after the amendment (day 3, 6, 8, 10, and 13). Water samples were filtered through 0.2 μm Whatman Polycap 36 AS nylon membrane cartridge filters to remove particulate matter, plankton and bacteria, using a Masterflex L/S Digital Standard Drive peristaltic pump with Easy Load II and Masterflex L/S 17 silicone tubing at 100 mL min⁻¹, directly into precleaned 10 L polyethylene Hedwin Cubitainers™. Filtered sample waters were stored in the dark in an environmental chamber set at temperatures matching the *in situ* temperatures of the JOMEX site before use. Sample waters were used in photoirradiation experiments at the TZS within two days of collection. CDOM absorbance and DOC concentrations were measured for these experiments. Aliquots of remaining water samples were shipped on ice to the Skidaway Institute of Oceanography (SkIO), Savannah GA, USA, and were stored in the dark at 4 °C before use; two more photoirradiation experiments were run on these shipped samples on 18 September and 24 September 2019. CDOM absorbance and photoproduct dissolved inorganic carbon concentrations were measured during these two additional experiments.

All plastic containers, filters, tubing and other labware for sampling and photoirradiation experiments were acid cleaned; first rinsed with copious amount of MilliporeSigma 18.2-M Ω .cm Milli-Q[®] Type 1 ultrapure water (Milli-Q water), then soaked overnight in 0.1 % HCl solution (pH 2). After rinsing again with an excess of Milli-Q water, these were stored with a small amount of fresh pH-2 HCl solution to prevent bacterial growth. Before use, plasticware were again rinsed with copious amounts of Milli-Q water. All glassware was acid washed following the same procedure, then dried and baked at 450 °C for at least 5 h. All labware was rinsed three times with a small volume of sample water prior to use. All acid solutions were made using Fisher Chemical Certified ACS Plus grade HCl and Milli-Q water.

Photoirradiation experiment: Photoirradiation experiments were carried out following the protocols described in Powers et al. (2017) (53). Samples from the control, humic-amended, and humic+nutrients-amended mesocosms were each partitioned into 6 10-cm-pathlength cylindrical Spectrocell spectrophotometric quartz cells (cells, ~30 mL volume each). These quartz cells and caps were cleaned following abovementioned protocols but not baked at 450 °C. Each cell was rinsed 3 times with sample water from the corresponding cubitainers before filling, without headspace, directly from the cubitainers. Each cell was capped with two Spectrocell caps fitted with Microsolv Teflon-lined butyl septa. Five cells for each treatment type (15 total) were placed vertically into a temperature (15°C) controlled black aluminum block, and irradiated under an Atlas Suntest CPS+ solar simulator equipped with a 1.5 kW xenon lamp (54, 53, 55). The solar simulator was fitted with a daylight filter (excluding light below ~300 nm) to provide the cells with precisely known, full spectral light. One cell for each treatment type was wrapped in aluminum foil to serve as dark control and placed in the same water bath that provided cooling water to the aluminum block.

After irradiation, for each time point (irradiation time points see Table 1), 20 mL aliquots of the sample were collected from the quartz cells into acid-cleaned and 450 °C-baked 24-mL Shimadzu DOC vials, acidified to pH 2 and capped with Teflon-septa-lined caps. These samples were stored in the dark at 4 °C until analyzed within a week for DOC concentrations by high temperature catalytic oxidation method using a Shimadzu TOC-V CPH analyzer equipped with a Shimadzu ASI-V autosampler (56, 57) at the TZS.

To provide some background photodegradation rates of added humic substances, the same Humintech GmbH HuminFeed® WSG was dissolved in Milli-Q water at a concentration of 2 mg L⁻¹, filtered through a 0.2 µm Whatman Polycap 36 AS nylon membrane cartridge filter the same way the mesocosm samples were filtered, and irradiated in a similar fashion in temperature controlled quartz cells under the solar simulator. DOC concentrations were determined within a week using a Shimadzu TOC-V CPH analyzer at SkIO using similar protocols as describe above.

<Table 1>

Optical measurements and analyses: After DOC samples were collected, absorbance ($A(\lambda)$) in the remaining sample waters were measured at 250 - 800 nm at 1.0 nm intervals, in duplicate, in a 1-cm-pathlength quartz spectrophotometric cuvette. At TZS, a Shimadzu UV-2501PC UV-VIS recording spectrophotometer with UV-Probe software was used, with air as an internal reference, and Milli-Q water as blanks. At SkIO, absorbances were obtained using an Agilent 8453 UV-visible spectrophotometer with ChemStation software, with the same parameters as above, and Milli-Q water as blanks. The average absorbance spectra of blanks were subtracted from the absorbance spectra of the sample water. Absorbance spectra were further corrected for potential offsets and instrument drift by subtracting the average absorbance at 690 - 710 nm (58), before converting $A(\lambda)$ to Napierian absorption coefficients ($a_g(\lambda)$; m⁻¹), using the following equation (59): $a_g(\lambda) = \frac{A \ln 10}{L}$, where L (m) is the pathlength.

For laboratory irradiation experiments, the spectral downwelling irradiance $E_o(\lambda)$ (mol photons m⁻² s⁻¹ nm⁻¹) entering each cell was quantified using an Optronic Laboratories OL756 Portable UV-Vis Spectroradiometer. The calibration of the spectroradiometer, measurements of irradiance, and calculations of the photon dose absorbed by CDOM in the samples ($Q_a(\lambda)$, mol photons s⁻¹ nm⁻¹, equation 1), and wavelength (280 - 600 nm) integrated photon dose $Q_a(int)$ (mol photons absorbed, equation 2) were calculated following Powers et al. (2017) (53) and Hu et al. (2002) (60).

$$Q_a(\lambda) = E_o(\lambda)(1 - e^{-a_g(\lambda)L})S \quad (1)$$

where S (m²) is the area of the irradiated surface of the cells.

$$Q_a(int) = t \int_{280}^{600} Q_a(\lambda) \quad (2)$$

where t (s) is the irradiation time.

The *in situ* wavelength- (380 - 490 nm) and depth- (3 m) integrated photon dose ($Q_a(int)$, mol photons absorbed) was estimated following Fichot and Miller (2010) (61), using CDOM absorption measured during the LightCycle experiment ($a_g(\lambda)$ in unirradiated samples), diffuse attenuation coefficients estimated from measured absorption coefficients, and downwelling irradiance estimated from modeled data. Briefly, the diffuse attenuation coefficients (K_d) at 412 nm were estimated using measured a_g at 400 nm (equation in Figure 5 of Kowalczyk et al. 2005 (62): $\log(a_g(400)) = -0.0113 + 0.713 \times \log(K_d(412))$), and approximation ratios (control: 0.6 - 0.9; humic-amended: 0.6 - 0.7, humic+nutrients-amended: 0.5 - 0.6) were calculated by dividing $a_g(412)$ by $K_d(412)$.

Assuming that the contribution to K_d from CDOM absorption is consistent across the whole spectrum, K_d values across the 290 - 490 nm wavelength range were calculated by dividing the a_g values at corresponding wavelengths by these approximation ratios for the corresponding day. Cloud-corrected daily integrated downwelling irradiance (280 - 700 nm at 1 nm intervals) just below the water surface for July 15th (1996 - 2003) at 59.94 N, 23.26 E was calculated as described previously (61) using clear-sky downwelling irradiance obtained from the radiative transfer model STAR (System for Transfer of Atmospheric Radiation, (63)) and corrections for clouds. The *in situ* photon dose was integrated from 380 nm because the acrylic cover likely cut off all UV transmission below 380 nm.

CDOM fading in laboratory experiments were expressed as a_g fading rates (m^{-1} (mol photons absorbed)⁻¹), calculated by linear regressions of $a_g(\lambda)$ versus $Q_a(int)$. Similarly, the *in situ* a_g fading rates (m^{-1} (mol photons absorbed)⁻¹) were calculated by linear regressions of *in situ* $a_g(\lambda)$ (values in unirradiated samples from each day's laboratory experiment) versus *in situ* $Q_a(int)$. Laboratory a_g fading rates at 280 and 400 nm were selected as examples of the magnitude and changes of these fading rates, because CDOM absorbs most strongly at the UV range and absorption above 400 nm was very low. In case the changes in a_g differ between lower and higher wavelengths, the sum of total absorption at 280 - 400 nm (64) was calculated as integrated a_g across 280 - 400 nm ($a_g(int)$, m^{-1} nm) following the Simpson's Rule. $a_g(int)$ fading rates by photon dose (m^{-1} nm (mol photons absorbed)⁻¹) were calculated from linear regressions of $a_g(int)$ versus laboratory and *in situ* photon doses respectively, to provide an idea of the total amount of CDOM fading occurring in the UV range. To account for the possibility of other *in situ* CDOM loss mechanisms, such as flocculation and

biodegradation, the *in situ* a_g fading rates versus time ($\text{m}^{-1} \text{day}^{-1}$ and $\text{m}^{-1} \text{nm day}^{-1}$) were also calculated (by linear regressions of *in situ* $a_g(\lambda)$ and $a_g(\text{int})$ versus time (day)) to provide a general idea of CDOM loss in the mesocosms.

Chromophoric dissolved organic matter absorption spectral slope $S_{275-295}$ (nm^{-1}) values, which may reflect the molecular weights of CDOM molecules, were calculated by linear regressions of natural-log-transformed absorbance ($\ln A$) versus wavelength for 275 - 295 nm (65). Specific ultraviolet absorbance at 254 nm ($SUVA_{254}$; $\text{L mg}^{-1} \text{m}^{-1}$) has been correlated to DOM aromaticity of standard reference materials, and was calculated as the Decadic absorption coefficient at 254 nm ($A(254)/L$; m^{-1}) divided by DOC concentrations (mg L^{-1}) (66).

The laboratory rates of change of $S_{275-295}$ ($\text{nm}^{-1} (\text{mol photons absorbed})^{-1}$) and $SUVA_{254}$ ($\text{L mg}^{-1} \text{m}^{-1} (\text{mol photons absorbed})^{-1}$) were calculated using linear regressions of $S_{275-295}$ and $SUVA_{254}$ versus photons absorbed. The *in situ* values of these two parameters were from unirradiated samples in individual laboratory experiments, and the *in situ* rates of change ($\text{nm}^{-1} (\text{mol photons absorbed})^{-1}$, $\text{nm}^{-1} \text{day}^{-1}$, and $\text{L mg}^{-1} \text{m}^{-1} (\text{mol photons absorbed})^{-1}$, $\text{L mg}^{-1} \text{m}^{-1} \text{day}^{-1}$, respectively) were calculated using linear regressions of the *in situ* values versus *in situ* photon dose and time.

Dissolved inorganic carbon (DIC) measurements: Dissolved inorganic carbon photoproduction rates were measured at SkIO using a stable isotope dilution method, moderate dissolved inorganic carbon (DI^{13}C) isotope enrichment (MoDIE) (53). Briefly, water samples were enriched to about 5000 ‰ $\delta^{13}\text{C}$ -DIC using $\sim 7 \text{ mg L}^{-1}$ of $\text{NaH}^{13}\text{CO}_3$, equilibrated by stirring for at least 1 hour and then distributed to quartz cells using gas-sampling techniques (53) and irradiated as mentioned above. Samples were then injected into a ThermoFisher Delta V+ Isotope Ratio Mass Spectrometer through an ThermoFisher Isolink interface (67), and the $\delta^{13}\text{C}$ -DIC and initial DIC concentrations of the samples were measured. The concentrations of photochemically produced DIC (M) were then calculated using mass balances of DIC and $^{13}\text{C}/^{12}\text{C}$ (53). The DIC photoproduction rates P_{DIC} ($\mu\text{M} (\text{mmol photons absorbed})^{-1}$) were calculated using linear regressions of photochemically produced DIC concentrations (M) versus photons absorbed (mol). Integrated DIC photoproduction efficiencies (DIC apparent quantum yield, $\text{AQY}(\text{int})$; $\mu\text{mol} (\text{mol photons absorbed})^{-1}$) were calculated by multiplying P_{DIC} by the average quartz cell volume (30 mL).

Statistics: Linear regressions were performed using *lm* in R (68). Analysis of covariance (ANCOVA, *anova* in R; (68)) was used to determine whether the rates of change (slopes of linear regressions) in various parameters (over photons absorbed and time) were different among the different treatment types. When the slopes were not statistically different between treatment groups (ANCOVA interaction term $p > 0.05$), comparison of parameter values were made between different treatment groups using analysis of variance (ANOVA, *anova* in R; (68)) after adjusting for photon doses or time.

RESULTS

Chromophoric dissolved organic matter (CDOM) losses in the mesocosm

The humic and humic+nutrients-amended mesocosms had higher absorption coefficient values than the control mesocosm at the beginning of the amendment experiment due to the added humic substances (Table 1 and Figure S1, Supporting Information). This trend of higher a_g values in the amended mesocosms continued throughout the amendment experiment, but the a_g values decreased over time *in situ* in all mesocosms (Figs. 1, 2, and Figure S1, Supporting Information). By day 13, absorption coefficients were more similar between all three mesocosms (Table 1 and Figure S1, Supporting Information), corresponding to 7.8 % $a_g(280)$ and 4.2 % $a_g(400)$ losses in the control mesocosm, 20 % $a_g(280)$ and 42 % $a_g(400)$ losses in the humic-amended mesocosm, and 22 % $a_g(280)$ and 40 % $a_g(400)$ losses in the humic+nutrients-amended mesocosm. Similarly, the amended mesocosms had higher integrated absorption across the UV wavelength range of 280 - 400 nm (Fig. 1e, 1f, Table 1, and Figure S1, Supporting Information). Integrated absorption similarly decreased in all mesocosms (linear regressions, $p < 0.05$), corresponding to 10 %, 31 %, and 31 % losses in the control, humic- and humic+nutrients-amended mesocosms, respectively (Fig. 1e, 1f, Table 2, and Figure S1, Supporting Information).

<Figure 1>

<Figure 2>

The *in situ* integrated photon doses from 380 - 490 nm for humic- and humic+nutrients-amended samples were 80 - 93 % of those absorbed by control samples, due to the higher attenuation

coefficients in the amended mesocosms, which in turn was due to the higher absorption coefficients (Fig. 1a, 1c, and 1e). The *in situ* photon doses were similar between the humic- and humic+nutrients-amended samples. Despite the relatively smaller amounts of photons absorbed, a_g fading rates (slopes of linear regressions for a_g versus *in situ* photon dose) were much higher in the humic-amended mesocosm than in the control mesocosm (ANCOVA and linear regressions, $p < 0.05$), at 280 nm and 400 nm, and for $a_g(int)$ (Fig. 1, Table 2, and Figure S1, Supporting Information). There was no statistically significant difference in a_g fading rates between the humic- and humic+nutrients-amended samples at either wavelength or the integrated absorption (ANCOVA, $p > 0.05$. Fig. 1, Table 2, and Figure S1, Supporting Information).

Because it is not possible to separate the various CDOM loss and addition mechanisms that can potentially occur *in situ*, CDOM loss rates were also calculated versus sampling time in days (Fig. 1b, 1d, 1f, and Figure S1, Supporting Information). The trends of a_g fading rates versus time were similar to the trends in fading rates by photon dose, even though the rates were in units of $m^{-1} day^{-1}$ (Fig. 1 and Figure S1, Supporting Information). a_g fading rates were higher in the humic-amended mesocosm than in the control mesocosm (ANCOVA and linear regressions, $p < 0.05$, except for a non-significant slope of control sample at 400 nm. $a_g(280)$ fading rates for the control and humic-amended mesocosms were -0.11 ± 0.010 and $-0.38 \pm 0.030 m^{-1} day^{-1}$, respectively; $a_g(400)$ fading rates for the control and humic-amended mesocosms were -0.012 ± 0.0080 and $-0.095 \pm 0.0092 m^{-1} day^{-1}$, respectively Fig. 1b and 1d). However, there was no statistically significant difference in a_g fading rates versus time between the humic- and humic+nutrients-amended mesocosms at either wavelength (ANCOVA, $p > 0.05$. linear regressions, -0.42 ± 0.041 and $-0.089 \pm 0.012 m^{-1} day^{-1}$ at 280 and 400 nm respectively for the humic+nutrients-amended mesocosm, $p < 0.05$, Fig. 1b and 1d). Similarly, $a_g(int)$ fading rates were higher in humic- ($-27 \pm 1.8 m^{-1} nm day^{-1}$) and humic+nutrients-amended mesocosms ($-27 \pm 2.7 m^{-1} nm day^{-1}$) than in the control mesocosm ($-6.0 \pm 0.60 m^{-1} nm day^{-1}$. ANCOVA and linear regressions, $p < 0.05$, Fig. 1f) but were not significantly different between the amended mesocosms (ANCOVA, $p > 0.05$).

CDOM losses during laboratory irradiation experiments

For laboratory irradiation experiments, amended samples had higher CDOM absorption coefficients at 280 and 400 nm than control samples throughout each experiment, and the same trend was also seen in the 280 - 400 nm integrated absorption $a_g(int)$ (ANCOVA and ANOVA, $p < 0.05$. Figure S2, Supporting Information). Between the amended samples, humic-amended samples had higher $a_g(280)$ and $a_g(int)$ than the humic+nutrients-amended samples in irradiation experiments conducted using the day 10 and 13 samples, and higher $a_g(400)$ in day 13 samples (ANCOVA and ANOVA, $p < 0.05$), humic+nutrients-amended samples had higher $a_g(400)$ in day 1 samples, but otherwise the a_g values were not statistically different between the two groups during irradiation experiments (ANCOVA and ANOVA, $p > 0.05$. Figure S2, Supporting Information).

At the beginning of the amendment experiment, the amended samples absorbed more photons than the control samples in laboratory irradiation experiments because of the higher CDOM absorption, at about twice as high on day 1. This difference decreased over time, and towards the end of the amendment experiment, the photons absorbed during laboratory irradiation experiments were similar among all three groups (Fig. 3 and Figures S2 and S3, Supporting Information). Chromophoric dissolved organic matter faded in laboratory irradiation experiments, as indicated by the consistent decreases of absorption $a_g(280)$ and $a_g(int)$ with Figures S2 and S3, Supporting Information, photon dose, for all treatment groups for all experimental days (linear regressions, $p < 0.05$, Fig. 3, Table 2, and Figures S2 and S3, Supporting Information). The changes in $a_g(400)$ were more variable, some days there was fading (linear regressions, $p < 0.05$), but there were no statistically significant changes in $a_g(400)$ with photon dose in day 1, 3, and 10 control samples and day 3, 10, and 13 humic-amended samples (linear regressions, $p \geq 0.05$, Fig. 3, Table 2, and Figures S2 and S3, Supporting Information).

At 280 nm, the a_g fading rates (slopes of regression lines for a_g versus photon dose) in the control samples were higher than those in the humic-amended samples for most of the amendment experiment (ANCOVA and linear regressions, $p < 0.05$), except for day 8 and day 13 when there was no difference between the two groups (ANCOVA, $p > 0.05$, Fig. 3a, 3d and 3g, Table 2, and Figures S2 and S3, Supporting Information). The a_g fading rates at 400 nm were not statistically different in the humic-amended and control samples for all days (ANCOVA, $p > 0.05$, Fig. 3b, 3e and 3h, Table 2, and Figures S2 and S3, Supporting Information). The humic+nutrients-amended samples had similar a_g fading rates to the humic-amended samples, for all days at 280 nm and 400 nm (ANCOVA, $p >$

0.05), except that the humic+nutrients-amended samples faded faster at 400 nm than the humic-amended sample on day 3 (ANCOVA and linear regressions, $p < 0.05$. Fig. 3, Table 2, and Figures S2 and S3, Supporting Information). Integrated absorption $a_g(int)$ faded faster in the control samples on day 1, and in the humic+nutrients-amended samples on day 13 (ANCOVA and linear regressions, $p < 0.05$), but otherwise the fading rates in $a_g(int)$ were not statistically different among groups (ANCOVA, $p \geq 0.05$, Fig. 3c, 3f, and 3i, Table 2, and Figures S2 and S3, Supporting Information).

For $a_g(280)$, $a_g(400)$, and $a_g(int)$, the fading rates in individual irradiation experiments were variable across sampling days, and about 3-5 orders of magnitudes higher than the *in situ* rates in all groups (Table 2). In addition, the a_g fading rates in laboratory irradiation experiment of HuminFeed in Milli-Q water was $-445.58 \pm 52.317 \text{ m}^{-1}$ (mol photons absorbed) $^{-1}$ at 280 nm, $-188.80 \pm 37.097 \text{ m}^{-1}$ (mol photons absorbed) $^{-1}$ at 400 nm, and $-41557 \pm 5461.3 \text{ m}^{-1} \text{ nm}$ (mol photons absorbed) $^{-1}$ for $a_g(int)$ (Table 2). The $a_g(400)$ and $a_g(int)$ fading rates of HuminFeed in Milli-Q water were comparable to the laboratory a_g fading rates of humic-amended mesocosm samples, but were only about half of the average laboratory a_g fading rates of humic-amended mesocosm samples at 280 nm (Table 2).

<Figure 3>

<Table 2>

Changes in CDOM spectral slopes ($S_{275-295}$) in the mesocosms and during laboratory experiments

The control mesocosm had higher initial $S_{275-295}$ values (0.024 nm^{-1}) than the amended mesocosms (0.020 and 0.021 nm^{-1} for humic- and humic+nutrients-amended mesocosms, respectively). This trend of higher $S_{275-295}$ values in the control mesocosm than in the amended mesocosms continued throughout the amendment experiment. $S_{275-295}$ values increased *in situ* with photon dose and time in the amended mesocosms (linear regressions, $p < 0.05$), but showed no statistically significant changes with photon dose or time in the control mesocosm (linear regression, $p \geq 0.05$, Fig. 4). As a result, rates of change in $S_{275-295}$ values (slopes of linear regressions for $S_{275-295}$ versus *in situ* photon dose) were higher in the humic-amended mesocosm ($5.6 \times 10^{-5} \pm 6.5 \times 10^{-6} \text{ nm}^{-1}$ (mol photons absorbed) $^{-1}$ and $2.9 \times 10^{-4} \pm 3.6 \times 10^{-5} \text{ nm}^{-1} \text{ day}^{-1}$, linear regressions, $p < 0.05$) than in the control mesocosm (1.8

$\times 10^{-5} \pm 6.6 \times 10^{-6} \text{ nm}^{-1} (\text{mol photons absorbed})^{-1}$ and $1.0 \times 10^{-4} \pm 4.3 \times 10^{-5} \text{ nm}^{-1} \text{ day}^{-1}$, linear regressions, $p < 0.05$) (ANCOVA, $p < 0.05$, Fig. 4). The $S_{275-295}$ values were not statistically different between the two amended mesocosms for the duration of the amendment experiment, and the rates of change in $S_{275-295}$ values were not statistically different between the two groups (ANCOVA and ANOVA, $p > 0.05$). $5.5 \times 10^{-5} \pm 7.9 \times 10^{-6} \text{ nm}^{-1} (\text{mol photons absorbed})^{-1}$ and $2.8 \times 10^{-4} \pm 4.2 \times 10^{-5} \text{ nm}^{-1} \text{ day}^{-1}$ for humic+nutrients-amended mesocosm, linear regressions, $p < 0.05$, Fig. 4). At the end of the amendment experiment (day 13), $S_{275-295}$ values increased by 18 % in the humic-amended mesocosm and 16 % in the humic+nutrients-amended mesocosm, and these values became more similar to that in the control mesocosm than at the beginning of the amendment experiment.

<Figure 4>

In individual irradiation experiments, $S_{275-295}$ increased with photon dose in most treatment groups on most days sampled (linear regressions, $p < 0.05$), except on day 3 there was no change in the humic-amended samples (linear regression, $p \geq 0.05$, Fig. 5 and Figure S4, Supporting Information). However, it is possible that the missing data point in humic-amended samples on day 3 lead to reduced statistical power and the difference in slopes on day 3 needs to be interpreted with caution. On day 10 there was no change in the control and humic-amended samples, and on day 13 there was no change in the humic-amended samples (linear regressions, $p \geq 0.05$, Figure 5 and Figure S4, Supporting Information).

In day 1 and 6 samples, the rates of change in $S_{275-295}$ (slopes of linear regressions for $S_{275-295}$ versus photon dose) were higher in the control samples than in the humic-amended samples, and on day 3 the rate was higher in the humic+nutrients-amended than in the humic-amended samples (ANCOVA and linear regressions, $p < 0.05$, Fig. 5). For the rest of the samples, the rates of change in spectral slopes were not different between control and humic-amended samples, or between humic and humic+nutrients-amended samples (ANCOVA, $p \geq 0.05$, Fig. 5 and Figure S4, Supporting Information).

<Figure 5>

Dissolved organic matter (DOM) degradation

The initial after-amendment DOC concentrations were 5.2, 5.5, and 6.3 mg L⁻¹ for control, humic-amended, and humic+nutrients-amended mesocosms, respectively (Figure 6 and Table 1). DOC concentrations were higher in the humic-amended mesocosm than those in the control mesocosm at the beginning and over the course of the amendment experiment (ANOVA, $p < 0.05$, Fig. 6). DOC concentrations decreased *in situ* in both the control and humic-amended mesocosms with photon dose and time (-0.0064 ± 0.0015 mg L⁻¹ (mol photons absorbed)⁻¹ and -0.038 ± 0.0085 mg L⁻¹ day⁻¹ in the control mesocosm, and 0.0073 ± 0.0017 mg L⁻¹ (mol photons absorbed)⁻¹ and -0.038 ± 0.0090 mg L⁻¹ day⁻¹ in the humic-amended mesocosm. Linear regressions, $p < 0.05$), although there was no statistically significant difference between the rates of change (ANCOVA, $p = 0.7$). DOC concentrations in the humic+nutrients-amended mesocosm were highly variable *in situ* over the course of the amendment experiment, and this variability precluded the evaluation of *in situ* DOM degradation rates based on DOC values in these samples, or comparison to other treatments.

In laboratory irradiation experiments, no clear trends in DOC concentration changes were detected (data not shown), because either changes in DOC concentrations were smaller than the signal to noise level of the Shimadzu TOC analyzer, or the DOC concentrations fluctuated a lot over the course of the irradiation but were not significantly different before and after irradiation, so that it was impossible to calculate the photodegradation rates of DOM directly, or to make comparisons among the different treatments for laboratory experiments.

The initial DOC concentration of HuminFeed in Milli-Q water (2 mg L⁻¹) was 0.30 ± 0.033 mg L⁻¹. This concentration is consistent with the difference between the initial DOC concentrations in control and humic-amended mesocosms. There was no consistent change in DOC concentrations with photon dose when the HuminFeed in Milli-Q water samples were irradiated (linear regression, $p = 0.4$).

<Figure 6>

The initial after-amendment specific ultraviolet absorbance at 254 nm ($SUVA_{254}$) values were 2.1, 2.4, and 2.1 L mg⁻¹ m⁻¹ for control, humic-amended, and humic+nutrients-amended mesocosms, respectively (Figure 7 and Table 1). The *in situ* $SUVA_{254}$ values were higher in the humic-amended mesocosm than in the control mesocosm at the beginning and throughout the amendment experiment (ANOVA, $p < 0.05$, Fig. 7). $SUVA_{254}$ decreased in the humic-amended mesocosm with photon dose and time (-0.0038 ± 0.00088 L mg⁻¹ m⁻¹ (mol photons absorbed)⁻¹ and -0.020 ± 0.0047 L mg⁻¹ m⁻¹

day⁻¹. Linear regressions, $p < 0.05$), but there was no change in $SUVA_{254}$ values in the control mesocosm (linear regressions, $p > 0.05$) (Figure 7a and 7b). As a result, the rates of change were higher in the humic-amended mesocosm with both photon dose and time (ANCOVA, $p < 0.05$). The $SUVA_{254}$ value in the humic-amended mesocosm ($2.2 \text{ L mg}^{-1} \text{ m}^{-1}$) became more similar to that in the control mesocosm ($2.1 \text{ L mg}^{-1} \text{ m}^{-1}$) at the end of the amendment experiment. $SUVA_{254}$ values in the humic+nutrients-amended mesocosm were again highly variable over the course of the amendment experiment, and this variability precluded the calculation of a linear rate, or comparison to other treatments.

In laboratory irradiation experiments, the changes in $SUVA_{254}$ values with photon dose fluctuated over the course of the amendment experiment. $SUVA_{254}$ values decreased with photon dose in the control and humic+nutrients-amended samples on day 6, 8, and 13, decreased in the humic-amended samples on day 8 only (linear regressions, $p < 0.05$), and otherwise showed no changes with photon dose (linear regressions, $p \geq 0.05$) (Figure 7c-f and Figure S5, Supporting Information). The rates of change were not different among the treatments (ANCOVA, $p \geq 0.05$) except for day 6, when the rate of change was higher in control than in the humic-amended samples (ANCOVA, $p < 0.05$) (Figure 7c-f).

The initial $SUVA_{254}$ of HuminFeed in Milli-Q water was $10 \pm 2.3 \text{ L mg}^{-1} \text{ m}^{-1}$. There was no consistent change in $SUVA_{254}$ values with photon dose when the samples were irradiated (linear regression, $p = 0.4$).

<Figure 7>

Although direct measurement of DOM photodegradation rates in laboratory experiments proved impossible given the variability of the DOC concentrations, DIC photoproduction rates measured using the MoDIE method provided some clue to the rates of DOM photodegradation in the treatment groups and the changes in these rates. Immediately after amendment (day 1), all groups had similar DIC photoproduction rates, at $1.4 \pm 0.089 \mu\text{M (mmol photons absorbed)}^{-1}$ ($\text{AQY(int)} = 43 \pm 2.7 \mu\text{mol DIC (mol photons absorbed)}^{-1}$) for control samples, $1.5 \pm 0.11 \mu\text{M (mmol photons absorbed)}^{-1}$ ($\text{AQY(int)} = 44 \pm 3.4 \mu\text{mol DIC (mol photons absorbed)}^{-1}$) for humic-amended samples, and $1.6 \pm 0.17 \mu\text{M (mmol photons absorbed)}^{-1}$ ($\text{AQY(int)} = 48 \pm 5.1 \mu\text{mol DIC (mol photons absorbed)}^{-1}$) for humic+nutrients-amended samples, respectively (Figure 8). By day 6, the rates in control and humic-

amended samples increased to $2.7 \pm 0.23 \mu\text{M (mmol photons absorbed)}^{-1}$ ($\text{AQY(int)} = 82 \pm 6.8 \mu\text{mol DIC (mol photons absorbed)}^{-1}$), and $2.5 \pm 0.11 \mu\text{M (mmol photons absorbed)}^{-1}$ ($\text{AQY(int)} = 74 \pm 3.3 \mu\text{mol DIC (mol photons absorbed)}^{-1}$), corresponding to 93 % increase and 67 % increase, respectively. The rate in humic+nutrients-amended samples remained the same ($1.6 \pm 0.15 \mu\text{M (mmol photons absorbed)}^{-1}$, $\text{AQY(int)} = 47 \pm 4.6 \mu\text{mol DIC (mol photons absorbed)}^{-1}$) (Figure 8).

In addition, the DIC photoproduction rate in the irradiation experiment of HuminFeed in Milli-Q water was $3.5 \pm 0.34 \mu\text{M (mmol photons absorbed)}^{-1}$ ($\text{AQY(int)} = 106 \pm 10 \mu\text{mol DIC (mol photons absorbed)}^{-1}$). This rate was over 2 times higher than the laboratory DIC photoproduction rates of humic-amended mesocosm samples on day 1.

<Figure 8>

DISCUSSION

CDOM losses during the mesocosm experiment and laboratory irradiation experiments

Humic- and humic+nutrients-amended mesocosm samples had higher initial a_g values (Figure 2, Table 1, and Figure S1, Supporting Information) and lower $S_{275-295}$ values (Figure 4), consistent with added humic substances leading to higher absorption and with observed browning effects in surface waters (13, 14). The amended samples absorbed less photons *in situ* than the control samples (Figure 1) despite the higher absorption, most likely due to the higher attenuation coefficients in the amended samples, so light decreased with depth much faster in the amended mesocosms. The higher attenuation in turn was likely due to the higher CDOM absorption from humic substance addition, but possible also from particle formation induced by the added HuminFeed (69), although the estimation of *in situ* light dose in this study assumed a constant contribution from CDOM absorption to attenuation. The decrease in light availability at depth caused by higher light attenuation is also consistent with the effect of browning on light availability in the water column (70).

CDOM absorption coefficients generally decreased over time *in situ* and in laboratory irradiation experiments (Figure 1, 2, 3, Table 2, and Figures S1, S2 and S3, Supporting Information), suggesting CDOM degradation *in situ* and by photoirradiation. The added humic substances led to changes in CDOM absorption fading rates, however the effect is different *in situ* and in laboratory irradiation

experiments of filtered samples. The *in situ* a_g fading rates of amended samples were higher than those of control samples even though the photon doses were lower in the amended mesocosms (Fig. 1, Table 2, and Figure S1, Supporting Information), whereas in laboratory experiments, control samples generally had higher a_g fading rates than the amended samples at 280 nm, and the fading rates were generally not different among all three groups for $a_g(400)$ and $a_g(int)$, with a few exceptions (Fig. 3, Table 2, and Figures S2 and S3, Supporting Information). If the dominant CDOM loss process *in situ* were photodegradation, we should have seen differences in rates similar to those in laboratory experiments when comparing the loss rates among different treatments. These results suggest that the *in situ* CDOM fading might not be entirely due to photodegradation, but have contributions from other processes such as biological degradation (71, 72, 69) or particle formation (69, 34, 33), especially considering the reduced light availability in the mesocosms because of the cut off of short-wavelength UV light by the acrylic cover.

The addition of humic substances seemed to lower the a_g fading rate in laboratory irradiation experiments, and this pattern was more pronounced at the lower UV range, e.g. at 280 nm. The slower a_g fading at the lower UV range may mean more UV protection for organisms from the added humic substances, while the impact on the availability of photosynthetically active radiation may still be significant. However, “recovery” to an original state of CDOM absorption might be faster at higher wavelengths in the visible.

When comparing the results from the laboratory irradiation experiment of HuminFeed in Milli-Q water to those from laboratory experiments of mesocosm samples, it is interesting that the a_g fading rates were similar at 400 nm and when integrated from 280 to 400 nm, but the rate at 280 nm in Milli-Q water was half that of the humic-amended mesocosm sample rate (Table 2). It is possible that much higher background CDOM fading rates at 280 nm in the humic-amended mesocosm samples, i.e. fading in the native mesocosm water comparable to control mesocosm samples (Fig. 3 and Table 2), contributed to this higher fading rate.

It is also worth noting, that the a_g fading rates in laboratory irradiation experiments were 3 to 5 orders of magnitude higher than the *in situ* a_g fading rates in all samples (Table 2). One possible explanation is that processes other than photochemistry are responsible for the CDOM removal *in situ*, as mentioned above, and the rates of these processes were lower than photodegradation (73, 74, 71).

The composition of the native and added CDOM/DOM likely played a role in the degradation rates. Their results were based on riverine DOM, but Benner and Kaiser (2011) found that while biodegradation is mainly responsible for the loss of total DOC and the amino acid components of DOM, CDOM and lignin phenols degrade faster photochemically (73). These results were consistent with our results of faster CDOM fading in laboratory irradiation experiments. Since allochthonous tDOM makes a significant contribution to the high molecular weight DOM pool in the surface Baltic Sea water (48), and tDOM frequently contains humic substances, such as lignin polyphenols (11), it would not be surprising that the mesocosm samples in this study contained a high percentage of lignin phenols, and led to faster photodegradation.

In addition, it is likely that while photodegradation was occurring *in situ*, the reduced wavelength range of solar radiation reaching the mesocosms led to more indirect photochemical loss, whereas full spectral solar irradiation in laboratory experiments could cause both direct and indirect photochemical degradation (75). The *in situ* integrated (290 - 490 nm) photon dose could be 23 - 25 % higher than the current estimated $Q_a(int)$, if there were no acrylic cover over the mesocosms. Other factors and processes will likely affect the *in situ* photodegradation of DOM (76-78), but high laboratory photodegradation rates suggests that there's a high potential for photodegradation of the added humic substances, at least of the colored portion. While the samples in our Baltic Sea study are different, previous work found very little degradation of HuminFeed when kept in the dark, but observed CDOM and DOC decreases accompanied by increases in particulate matter, when exposed to visible light (69).

It is also possible that CDOM is produced *in situ* by microbial activities (79), and thus CDOM degradation is counteracted by CDOM production and led to lowered net loss *in situ*. Without dark incubation experiments to measure biological degradation and/or production, it is not possible to separate the photochemical from the biological effects in the mesocosms or to determine the relative importance of photodegradation in removing the added humic substances.

There was no difference in CDOM loss rates between humic-amended and humic+nutrients amended samples *in situ* (Fig. 1, Table 2, and Figure S1, Supporting Information), suggesting that either nutrients did not enhance CDOM biodegradation or that biodegradation of HuminFeed DOM is not that important. Similarly, nutrient additions in general didn't affect CDOM fading in laboratory

irradiation experiments, suggesting that CDOM photodegradation is not affected or negligibly affected by nutrient additions.

Chromophoric dissolved organic matter absorption coefficients became similar in all treatments towards the end of the amendment experiment (Fig. 1), suggesting that the increase in color from the added humic substances diminished over time, and the mesocosms returned close to their original states at least in terms of color.

Changes in CDOM spectral slopes ($S_{275-295}$) in the mesocosms and during laboratory experiments

Spectral slopes were lower in amended samples than in control samples (Figs. 4, 5, and Figure S4, Supporting Information), likely due to the increased absorption from the addition of HuminFeed, but may also suggest an addition of higher molecular weight CDOM to the amended samples (65), as HuminFeed is characterized as having a high abundance of higher molecular weight aromatic compounds (69). Spectral slopes increased with photons absorbed and time in amended samples *in situ* and in laboratory irradiation experiments (with some exceptions) (Figs. 4, 5, and Figure S4, Supporting Information), suggesting *in situ* degradation and photobleaching of CDOM, and may suggest a decrease in molecular weight of CDOM as CDOM degraded (65).

Similar to the trends in *in situ* CDOM losses, the rate of change in CDOM spectral slopes were higher in the humic-amended mesocosm than in control, but there were no differences between the two amended mesocosms (Fig. 4). In comparison, in laboratory experiments, the rates of change in $S_{275-295}$ were mostly not different among treatments with a few exceptions (Fig. 5 and Figure S4, Supporting Information). The differences between the *in situ* and laboratory rates of change again supported the hypothesis that other processes might be responsible for the changes in optical properties and possibly in molecular weight in the mesocosms.

DOM degradation

The DOC concentration was higher in the humic-amended mesocosm than in the control mesocosm, and the difference in DOC concentrations at the beginning of the amendment experiment corresponded well with the DOC concentration of 2 mg L⁻¹ HuminFeed dissolved in Milli-Q water

(Fig. 6). This result supports that the added humic substance led to increased DOC concentration. DOC decreased *in situ* with photon dose and time in control and humic-amended samples (Fig. 6), suggesting *in situ* degradation of DOM, although the addition of humic substances didn't seem to change the rate of DOC degradation as the change rates were not different between control and humic-amended samples. Because there were no clear change patterns in laboratory irradiation experiments, the *in situ* DOC decreases occurred in the control and humic-amended mesocosms may be mainly due to processes other than photodegradation. The potential input and subsequent degradation of phytoplankton-origin DOM (8) may be responsible for the highly fluctuating change patterns in the humic+nutrients-amended mesocosm (Fig. 6), if phytoplankton blooms occurred in response to the nutrient additions.

There was no clear trend in DOC concentration changes in laboratory irradiation experiments. It is possible that the irradiation was not long enough for DOC concentrations to change significantly, as Moran et al. 2000 (31) showed that there were only 9.4 - 30.7 % DOC loss during their 6 - 70 day long-term irradiation experiment. The addition of humic substances or humic and nutrients didn't appear to change the photoreactivity of the DOM at the time scale tested, and this hypothesis is further supported by the lack of statistically significant change in DOC concentrations in the HuminFeed in Milli-Q water experiment. The nature of the native DOM in this Baltic Sea site likely play an important role in affecting the DOC concentration change in the photoirradiation experiments. The DOM molecules at this Baltic Sea site may contain relatively high proportion of unsaturated aliphatic compounds (77), and aliphatic compounds tend to be more photoresistant (80). In addition, large phytoplankton blooms can occur from spring to autumn in the Baltic Sea (77), so it would not be entirely surprising to find high concentrations of plankton DOM at this site, particularly in the nutrients added mesocosms. However, studies have found conflicting results for the photoreactivity of phytoplankton-sourced DOM and thus could also be a reason why DOM photodegradation showed no clear trend in this dynamic system. Obernosterer and Benner (2004) found that plankton DOM exposed to light showed no loss in DOC (81), but Johannessen et al. (2007) found that algal-derived DOM had higher photodegradation efficiency than river DOM did (82). Furthermore, it is possible that the mesocosms in this study also had complex changes in DOM composition due to *in situ* DOM addition and removal, as suggested by a previous CDOM addition study at the IGB LakeLab (Stella

Berger, personal communication), and *in situ* processing of DOM (78) may have changed the photoreactivity of DOM molecules to further complicate the matter. For example, cyanobacteria could produce extracellular and intracellular DOM that are not readily degraded by photoirradiation (83).

The humic-amended mesocosm had higher specific ultraviolet absorbance $SUVA_{254}$ than control, $SUVA_{254}$ values decreased in the humic-amended mesocosm, and the humic-amended samples had higher rate of decrease in *in situ* $SUVA_{254}$ values than the control samples, although there was no statistically significant change in $SUVA_{254}$ values in control samples over the course of the amendment experiment (Fig. 7 and Table 1). These trends were again consistent with the addition of humic substances to the mesocosm, and may suggest an increase in aromaticity when humic substance was added (66) and a decrease in aromaticity during subsequent *in situ* degradation of the added humic substance (84, 80), as HuminFeed is abundant in aromatic compounds (69). The $SUVA_{254}$ values became similar again between the control and humic-amended mesocosms towards the end of the amendment experiment (Fig. 7a and 7b). This pattern again may suggest a “recovery” from the added humic substances to the original state in terms of specific ultraviolet absorbance. $SUVA_{254}$ values in the humic+nutrients-amended mesocosm were fluctuating with time (Fig. 6), again may point to complex DOM changes brought on by a potential nutrients-induced phytoplankton bloom (8).

The response of $SUVA_{254}$ values with photon dose varied in laboratory irradiation experiments, there were decreases in some samples for some days, mostly in the control and humic+nutrients-amended samples, and in the second half of the amendment experiment (Fig. 7c-f and Figure S5, Supporting Information). These results again may be caused by the differences in photoreactivity of the mesocosm samples due to complex changes and *in situ* processing of DOM molecules (78). The general lack of change pattern in the humic-amended samples, lack of difference between the rates of change in the control and humic-amended samples, and no significant change in $SUVA_{254}$ values with photon dose in the HuminFeed in Milli-Q water experiment, point to the likelihood that the changes in $SUVA_{254}$ values in the control and humic+nutrients-amended samples were likely caused by other properties in the samples than humic-substance-addition. Nutrient-addition didn't appear to change the $SUVA_{254}$ values either because the specific ultraviolet absorbance changes in the control and humic+nutrients-amended samples seemed to track each other.

The DIC photoproduction rates at day 1 were similar among all samples (Fig. 8), even though the control samples had higher a_g fading rates (Fig. 3 and Table 2). The production rates increased in control and humic-amended samples at day 6 but remained the same in humic+nutrients-amended samples (Fig. 8), again not in total agreement with the higher a_g fading rates in the control samples (Fig. 3 and Table 2). In addition, while integrated AQY for control ($43 - 82 \mu\text{mol DIC (mol photons absorbed)}^{-1}$) in this mesocosm study is lower than that for estuarine water from the South Atlantic Bight ($128 \pm 3.43 \mu\text{mol DIC (mol photons absorbed)}^{-1}$, (53)), and integrated AQY for humic-amended samples ($44 - 75 \mu\text{mol DIC (mol photons absorbed)}^{-1}$) is lower than that for a dark water river (initial $a_g(325) = 129 \text{ m}^{-1}$, $279 \pm 14.0 \mu\text{mol DIC (mol photons absorbed)}^{-1}$, (53)), the difference is much larger between the integrated AQY values of humic-amended samples and the dark water river. Therefore, it is reasonable to hypothesize that photons absorbed in the samples may lead to other photochemically-induced changes in CDOM/DOM but not complete remineralization, and DOM source may have a large impact on changes in DOM photodegradation rates. In fact, chemical analysis of HuminFeed revealed that it is relatively low in carboxylic acid groups that can efficiently carry out photodecarboxylation reactions (85), when compared to fresh terrestrial DOM isolated using reverse osmosis (69), which could explain why the addition of HuminFeed seemed to have little influence on DIC photoproduction rate despite lowering the a_g fading rates.

It is interesting though that the DIC photoproduction rates almost doubled in the control and humic-amended samples from day 1 to day 6, but remained relatively constant in the humic+nutrients-amended samples. It is possible that similar natural processes in the control and humic-amended mesocosms caused the DIC photoproduction rates to increase, and the presence of added humic substances in the humic-amended mesocosm had little effect on this increase, but the addition of nutrients stimulated microbial growth and consumption of DOM (8) in the humic+nutrients-amended mesocosms. This DOM consumption may have decreased the photoreactivity of DOM in terms of DIC production over time. For example, changes in CDOM/DOM structures, such as consumption of low molecular weight carboxylic acids (86), could lead to fewer CDOM/DOM molecules capable of complete photooxidation to CO_2 (85).

It is reasonable to hypothesize that the trends and changes in DIC photoproduction reflected to some degree the negligible effect of humic addition on DOM photodegradation rates and the negative

effects of nutrient addition. However, it is important to keep in mind that DOM photodegradation could also lead to production of biolabile DOM molecules, such as low molecular weight compounds (42, 87, 47), instead of complete oxidation to CO₂, so that the actual DOM degradation rates could be much higher in both the control and the amended samples. Without further experiments to test the lability of photo-reacted DOM in this system, it is impossible to make complete quantitative estimates of the actual DOM photodegradation rates.

In addition, the DIC photoproduction rates were higher in the HuminFeed in Milli-Q water samples than in the humic-amended mesocosm samples. Properties of the background Baltic seawater, such as salinity (44, 76), may have affected the ability of the humic substances to produce DIC photochemically. It is especially interesting that the a_g fading rates in laboratory experiments of HuminFeed in Milli-Q water was about half that of the humic-amended mesocosm samples at 280 nm. This offers further support that DOM and CDOM photodegradation is complex in this dynamic system, especially with added humic substances. CDOM photobleaching doesn't completely equal to DOM photodegradation, and DOM photodegradation doesn't always lead to complete remineralization.

Even though the optical properties in the amended mesocosms seemed to be “recovering” to the “original” state, i.e., similar to the control samples, these “recoveries” don't necessarily mean complete remineralization of the added CDOM/DOM. Instead, the degraded CDOM/DOM and photoproduction of biolabile DOM molecules may have further impact to the ecosystem during and after the “recovery”. Previous works in lakes and rivers show that browning can impact phytoplankton and bacterial communities (17, 21, 22, 19, 24), and it is likely that some of these impacts are brought on by the alteration of the added DOM molecules, such as the production of biolabile DOM (44). This impact and the role of DOM photodegradation may also be the case in estuarine systems even if the light field and optics differs from lakes and rivers.

Readdress the hypotheses

From the results of our laboratory experiments, it is clear that rapid CDOM/DOM photodegradation can occur after the addition of allochthonous CDOM/DOM to the Baltic Sea. Yet, even in mesocosms with much of the UV radiation removed, the system seems to return to a “normal” state or “recover”

from the excess CDOM/DOM, i.e., the CDOM absorption, spectral slopes and specific ultraviolet absorbance values became similar to those in the control mesocosm towards the end of the amendment experiment. Our results agree with what Aarnos et al. found in their 2012 study that the combined DOC photomineralization and subsequent bacterial utilization of photoproduct labile DOM exceeds the annual river input of photoreactive DOC to the Baltic Sea (44). However, the relative contribution of photodegradation to added allochthonous CDOM/DOM degradation could not be determined from this study. Furthermore, it is important to keep in mind that HuminFeed differs in many ways from natural CDOM/DOM and degrades differently in natural water (69), and further tests are necessary to more completely address the impact of browning and photochemical removal of added CDOM/DOM on coastal environments.

Comparison of changes in CDOM and DOM properties between *in situ* and laboratory irradiation experiments give some indication that processes other than photodegradation may be responsible for degradation of added CDOM and DOM in the humic-amended mesocosms, even though photodegradation has a high potential for removal of added CDOM/DOM. Scharnweber et al. (2021) found that lake water with added HuminFeed had significantly higher rate of particle formation and that HuminFeed stimulated bacterial production in the presence of light (69), and these processes may be responsible for at least some of the CDOM and DOM changes we saw in our study. It is possible that the availability of full spectral solar radiation at this Baltic Sea site may lead to more photodegradation of the added humic substances, and change the relative contribution of photodegradation to added and native CDOM/DOM degradation with respect to other *in situ* processes.

The addition of nutrients didn't lead to any major differences in the optical properties and their change rates in humic+nutrients-amended samples when compared to those in the humic-amended samples, and therefore didn't seem to compound the effects of added humic substances on DOM optical properties in this experiment. However, nutrient addition seemed to cause the DOC concentration, specific ultraviolet absorbance and DIC photoproduction to fluctuate over time in the humic+nutrients-amended mesocosm. This trend was not observed in the control or humic-amended mesocosms. This phenomenon may have been caused by DOM addition or removal during any potential phytoplankton changes induced by the nutrient addition (8).

To better constrain the importance of photodegradation to added humic substances in this Baltic Sea ecosystem, future studies could include concurrent photoirradiation and dark incubation experiments, quantum yield experiments combined with *in situ* light measurements to better estimate *in situ* photodegradation/photoproduction rates, and use of mesocosm covers that allow full spectral solar radiation penetration. In addition, future studies to measure the changes in fluorescent dissolved organic matter of photoirradiated samples may also help to differentiate photodegradation from biological degradation (11). Compositional and structural studies of DOM using Fourier-transform ion cyclotron resonance mass spectrometry and nuclear magnetic resonance spectroscopy, respectively, to analyze samples before and after irradiation and over the course of the amendment experiment, may complement optical and DIC photoproduction measurements, and provide a more complete picture of the DOM changes after browning and photoirradiation of this Baltic Sea ecosystem.

ACKNOWLEDGEMENTS: The authors would like to thank the scientists and staff at Tvärminne Zoological Station and the JOMEX team for providing equipment and facilities, assisting experimental setup and sample collection. We also thank Jaana Koistinen at Tvärminne Zoological Station for DOC sample analysis. In addition, we would like to thank Lee Ann DeLeo for assistance with graphics. This work was supported by the Transnational Access Programme of the AQUACOSM project grant 731065 funded by the European Union's Horizon 2020 Research and Innovation Programme, and United States National Science Foundation chemical oceanography grant 1635618. This study has utilized research infrastructure facilities provided by FINMARI (Finnish Marine Research Infrastructure network).

SUPPORTING INFORMATION

Additional supporting information may be found online in the Supporting Information section at the end of the article:

Figure S1. Chromophoric dissolved organic matter absorption coefficient a), b), c) versus photon doses ($Q_a(int)$, mol photons absorbed), and d), e), f) versus time (day), for JOMEX amendment

experiment samples that reflect the *in situ* conditions, a) d) at 280 nm, $a_g(280)$, m^{-1} ; b) e) at 400 nm, $a_g(400)$, m^{-1} ; c) f) integrated from 280 nm to 400 nm $a_g(int)$, $m^{-1} nm$. Samples were taken right after the initial amendment (day 1), and around the same time in subsequent days. Solid lines - linear regression lines, dashed lines - 95 % confidence bands for the slopes of the regression lines.

Figure S2. Chromophoric dissolved organic matter absorption coefficients at a) d) g) j) m) p) 280 nm ($a_g(280)$, m^{-1}), b) e) h) k) n) q) 400 nm ($a_g(400)$, m^{-1}), and c) f) i) l) o) r) integrated over 280-400 nm ($a_g(int)$, $m^{-1} nm$) versus photon dose (mmol photons absorbed) for laboratory irradiation experiments conducted on mesocosm samples of the JOMEX experiment (day 1 was the day of initial amendment). Solid lines - linear regression lines, dashed lines - 95 % confidence bands for the slopes of the regression lines.

Figure S3. Ratios of chromophoric dissolved organic matter absorption coefficients at a) d) g) 280 nm ($a_g(280)_T : a_g(280)_{T0}$), b) e) h) 400 nm ($a_g(400)_T : a_g(400)_{T0}$), and c) f) i) integrated over 280-400 nm ($a_g(int)_T : a_g(int)_{T0}$) versus photon dose (mmol photons absorbed) for laboratory irradiation experiments conducted on mesocosm samples of the JOMEX experiment (day 1 was the day of initial amendment). Ratios were calculated by dividing the corresponding a_g ratio at time T by that at time T_0 . Solid lines - linear regression lines, dashed lines - 95 % confidence bands for the slopes of the regression lines.

Figure S4. Chromophoric dissolved organic matter absorption spectral slope $S_{275-295}$ (nm^{-1}) versus photon dose ($Q_a(int)$, mmol photons absorbed) for individual laboratory experiments, using samples of the JOMEX amendment experiment. Samples were taken right after the initial amendment (day 1). Solid lines - linear regression lines, dashed lines - 95 % confidence bands for the slopes of the regression lines. Error bars were ± 1 standard error for $S_{275-295}$ (linear regression slopes of natural-log-transformed absorbance versus wavelength at 275-295 nm).

Figure S5. Specific ultraviolet absorbance $SUVA_{254}$ ($L\ mg^{-1}\ m^{-1}$) versus photon doses ($Q_a(int)$, mmol photons absorbed) for laboratory irradiation experiments using samples of the JOMEX amendment experiment. Day 1 was the day of initial amendment. Solid lines - linear regression lines, dashed lines - 95 % confidence bands for the slopes of the regression lines.

REFERENCES

1. Hansell, D. A. and C. A. Carlson (1998) Deep-ocean gradients in the concentration of dissolved organic carbon. *Nature* **395**, 263-266.
2. Hansell, D. A., C. A. Carlson, D. J. Repeta and R. Schlitzer (2009) Dissolved organic matter in the ocean: a controversy stimulates new insights. *Oceanography* **22**, 202-211.
3. Williams, P. M. and E. R. M. Druffel (1987) Radiocarbon in dissolved organic matter in the central North Pacific Ocean. *Nature* **330**, 246-248.
4. Hedges, J. I. (1992) GLOBAL BIOGEOCHEMICAL CYCLES - PROGRESS AND PROBLEMS. *Mar. Chem.* **39**, 67-93.
5. Amon, R. M. W. and R. Benner (1996) Bacterial utilization of different size classes of dissolved organic matter. *Limnology and Oceanography* **41**, 41-51.
6. Kroer, N. (1993) Bacterial-growth efficiency on natural dissolved organic matter. *Limnology and Oceanography* **38**, 1282-1290.
7. Cherrier, J. and J. E. Bauer (2004) Bacterial utilization of transient plankton-derived dissolved organic carbon and nitrogen inputs in surface ocean waters. *Aquatic Microbial Ecology* **35**, 229-241.
8. Carlson, C. A. and D. A. Hansell (2015) Chapter 3 - DOM Sources, Sinks, Reactivity, and Budgets. *Biogeochemistry of Marine Dissolved Organic Matter*, 65-126.
9. Mayorga, E., S. P. Seitzinger, J. A. Harrison, E. Dumont, A. H. W. Beusen, A. F. Bouwman, B. M. Fekete, C. Kroeze and G. Van Drecht (2010) Global Nutrient Export from WaterSheds 2

(NEWS 2): Model development and implementation. *Environmental Modelling & Software* **25**, 837-853.

10. Aitkenhead, J. A. and W. H. McDowell (2000) Soil C : N ratio as a predictor of annual riverine DOC flux at local and global scales. *Glob. Biogeochem. Cycle* **14**, 127-138.
11. Coble, P. G. (2007) Marine optical biogeochemistry: The chemistry of ocean color. *Chemical Reviews* **107**, 402-418.
12. Blough, N. V. and R. Del Vecchio (2002) Chapter 10 - Chromophoric DOM in the Coastal Environment. In *Biogeochemistry of Marine Dissolved Organic Matter*. (Edited by D. A. Hansell and C. A. Carlson), pp. 509-546. Academic Press, San Diego.
13. de Wit, H. A., S. Valinia, G. A. Weyhenmeyer, M. N. Futter, P. Kortelainen, K. Austnes, D. O. Hessen, A. Raike, H. Laudon and J. Vuorenmaa (2016) Current Browning of Surface Waters Will Be Further Promoted by Wetter Climate. *Environ. Sci. Technol. Lett.* **3**, 430-435.
14. Monteith, D. T., J. L. Stoddard, C. D. Evans, H. A. de Wit, M. Forsius, T. Hogasen, A. Wilander, B. L. Skjelkvale, D. S. Jeffries, J. Vuorenmaa, B. Keller, J. Kopacek and J. Vesely (2007) Dissolved organic carbon trends resulting from changes in atmospheric deposition chemistry. *Nature* **450**, 537-U539.
15. Tranvik, L. J., J. A. Downing, J. B. Cotner, S. A. Loiselle, R. G. Striegl, T. J. Ballatore, P. Dillon, K. Finlay, K. Fortino, L. B. Knoll, P. L. Kortelainen, T. Kutser, S. Larsen, I. Laurion, D. M. Leech, S. L. McCallister, D. M. McKnight, J. M. Melack, E. Overholt, J. A. Porter, Y. Prairie, W. H. Renwick, F. Roland, B. S. Sherman, D. W. Schindler, S. Sobek, A. Tremblay, M. J. Vanni, A. M. Verschoor, E. von Wachenfeldt and G. A. Weyhenmeyer (2009) Lakes and reservoirs as regulators of carbon cycling and climate. *Limnology and Oceanography* **54**, 2298-2314.
16. Kritzberg, E. S., W. Graneli, J. Bjork, C. Bronmark, P. Hallgren, A. Nicolle, A. Persson and L. A. Hansson (2014) Warming and browning of lakes: consequences for pelagic carbon metabolism and sediment delivery. *Freshw. Biol.* **59**, 325-336.
17. Brothers, S., J. Kohler, K. Attermeyer, H. P. Grossart, T. Mehner, N. Meyer, K. Scharnweber and S. Hilt (2014) A feedback loop links brownification and anoxia in a temperate, shallow lake. *Limnology and Oceanography* **59**, 1388-1398.

18. Santonja, M., L. Minguéz, M. O. Gessner and E. Sperfeld (2017) Predator-prey interactions in a changing world: humic stress disrupts predator threat evasion in copepods. *Oecologia* **183**, 887-898.
19. Urrutia-Cordero, P., M. K. Ekvall, J. Ratcovich, M. Soares, S. Wilken, H. Zhang and L. A. Hansson (2017) Phytoplankton diversity loss along a gradient of future warming and brownification in freshwater mesocosms. *Freshw. Biol.* **62**, 1869-1878.
20. Vasconcelos, F. R., S. Diehl, P. Rodriguez, J. Karlsson and P. Bystrom (2018) Effects of Terrestrial Organic Matter on Aquatic Primary Production as Mediated by Pelagic-Benthic Resource Fluxes. *Ecosystems* **21**, 1255-1268.
21. Feuchtmayr, H., T. G. Pottinger, A. Moore, M. M. De Ville, L. Caillouet, H. T. Carter, M. G. Pereira and S. C. Maberly (2019) Effects of brownification and warming on algal blooms, metabolism and higher trophic levels in productive shallow lake mesocosms. *Sci. Total Environ.* **678**, 227-238.
22. Karlsson, J., P. Bystrom, J. Ask, P. Ask, L. Persson and M. Jansson (2009) Light limitation of nutrient-poor lake ecosystems. *Nature* **460**, 506-U580.
23. Deininger, A. and H. Frigstad (2019) Reevaluating the Role of Organic Matter Sources for Coastal Eutrophication, Oligotrophication, and Ecosystem Health. *Front. Mar. Sci.* **6**, 11.
24. Andersson, A., I. Jurgensone, O. F. Rowe, P. Simonelli, A. Bignert, E. Lundberg and J. Karlsson (2013) Can Humic Water Discharge Counteract Eutrophication in Coastal Waters? *PLoS One* **8**, e61293.
25. Lauerwald, R., J. Hartmann, W. Ludwig and N. Moosdorf (2012) Assessing the nonconservative fluvial fluxes of dissolved organic carbon in North America. *Journal of Geophysical Research-Biogeosciences* **117**, 19.
26. Osburn, C. L. and T. S. Bianchi (2016) Editorial: Linking Optical and Chemical Properties of Dissolved Organic Matter in Natural Waters. *Front. Mar. Sci.* **3**, 3.
27. Massicotte, P., E. Asmala, C. Stedmon and S. Markager (2017) Global distribution of dissolved organic matter along the aquatic continuum: Across rivers, lakes and oceans. *Sci. Total Environ.* **609**, 180-191.

28. Farjalla, V. F., A. M. Amado, A. L. Suhett and F. Meirelles-Pereira (2009) DOC removal paradigms in highly humic aquatic ecosystems. *Environ. Sci. Pollut. Res.* **16**, 531-538.
29. Moran, M. A., W. M. Sheldon and J. E. Sheldon (1999) Biodegradation of riverine dissolved organic carbon in five estuaries of the southeastern United States. *Estuaries* **22**, 55-64.
30. Asmala, E., R. Autio, H. Kaartokallio, C. A. Stedmon and D. N. Thomas (2014) Processing of humic-rich riverine dissolved organic matter by estuarine bacteria: effects of predegradation and inorganic nutrients. *Aquatic Sciences* **76**, 451-463.
31. Moran, M. A., W. M. Sheldon and R. G. Zepp (2000) Carbon loss and optical property changes during long-term photochemical and biological degradation of estuarine dissolved organic matter. *Limnology and Oceanography* **45**, 1254-1264.
32. Santos, L., E. B. H. Santos, J. M. Dias, A. Cunha and A. Almeida (2014) Photochemical and microbial alterations of DOM spectroscopic properties in the estuarine system Ria de Aveiro. *Photochemical & Photobiological Sciences* **13**, 1146-1159.
33. Sholkovitz, E. R. (1976) FLOCCULATION OF DISSOLVED ORGANIC AND INORGANIC MATTER DURING MIXING OF RIVER WATER AND SEAWATER. *Geochimica Et Cosmochimica Acta* **40**, 831-845.
34. Asmala, E., D. G. Bowers, R. Autio, H. Kaartokallio and D. N. Thomas (2014) Qualitative changes of riverine dissolved organic matter at low salinities due to flocculation. *Journal of Geophysical Research-Biogeosciences* **119**, 1919-1933.
35. Pinsonneault, A. J., P. J. Neale, M. Tzortziou, E. A. Canuel, C. R. Pondell, H. Morrissette, J. P. Megonigal and J. S. Lefcheck (2020) Dissolved organic carbon sorption dynamics in tidal marsh soils. *Limnology and Oceanography*, 12.
36. Chupakova, A. A., A. V. Chupakov, N. V. Neverova, L. S. Shirokova and O. S. Pokrovsky (2018) Photodegradation of river dissolved organic matter and trace metals in the largest European Arctic estuary. *Sci. Total Environ.* **622**, 1343-1352.
37. Bélanger, S., H. X. Xie, N. Krotkov, P. Larouche, W. F. Vincent and M. Babin (2006) Photomineralization of terrigenous dissolved organic matter in Arctic coastal waters from 1979 to 2003: Interannual variability and implications of climate change. *Glob. Biogeochem. Cycle* **20**, 13.

38. Dalzell, B. J., E. C. Minor and K. M. Mopper (2009) Photodegradation of estuarine dissolved organic matter: a multi-method assessment of DOM transformation. *Organic Geochemistry* **40**, 243-257.
39. Minor, E. C., B. L. Dalzell, A. Stubbins and K. Mopper (2007) Evaluating the photoalteration of estuarine dissolved organic matter using direct temperature-resolved mass spectrometry and UV-visible spectroscopy. *Aquatic Sciences* **69**, 440-455.
40. Osburn, C. L., L. Retamal and W. F. Vincent (2009) Photoreactivity of chromophoric dissolved organic matter transported by the Mackenzie River to the Beaufort Sea. *Mar. Chem.* **115**, 10-20.
41. Mopper, K. and D. J. Kieber (2000) Marine photochemistry and its impact on carbon cycling. In *The Effects of UV Radiation in the Marine Environment*. (Edited by M. Vernet, S. Demers and S. De Mora), pp. 101-129. Cambridge University Press, Cambridge.
42. Mopper, K., D. J. Kieber and A. Stubbins (2015) Marine Photochemistry of Organic Matter: Processes and Impacts. In *Biogeochemistry of Marine Dissolved Organic Matter, 2nd Edition*. (Edited by D. A. Hansell and C. A. Carlson), pp. 389-450. Academic Press Ltd-Elsevier Science Ltd, London.
43. Anderson, S., R. Zepp, J. Machula, D. Santavy, L. Hansen and E. Mueller (2001) Indicators of UV exposure in corals and their relevance to global climate change and coral bleaching. *Human and Ecological Risk Assessment* **7**, 1271-1282.
44. Aarnos, H., P. Ylostalo and A. V. Va'ha'talo (2012) Seasonal phototransformation of dissolved organic matter to ammonium, dissolved inorganic carbon, and labile substrates supporting bacterial biomass across the Baltic Sea. *Journal of Geophysical Research-Biogeosciences* **117**, 14.
45. Fichot, C. G. and R. Benner (2014) The fate of terrigenous dissolved organic carbon in a river-influenced ocean margin. *Glob. Biogeochem. Cycle* **28**, 300-318.
46. Miller, W. L. and M. A. Moran (1997) Interaction of photochemical and microbial processes in the degradation of refractory dissolved organic matter from a coastal marine environment. *Limnology and Oceanography* **42**, 1317-1324.

47. Miller, W. L., M. A. Moran, W. M. Sheldon, R. G. Zepp and S. Opsahl (2002) Determination of apparent quantum yield spectra for the formation of biologically labile photoproducts. *Limnology and Oceanography* **47**, 343-352.
48. Deutsch, B., V. Alling, C. Humborg, F. Korth and C. M. Morth (2012) Tracing inputs of terrestrial high molecular weight dissolved organic matter within the Baltic Sea ecosystem. *Biogeosciences* **9**, 4465-4475.
49. Carstensen, J., D. J. Conley, E. Almroth-Rosell, E. Asmala, E. Bonsdorff, V. Fleming-Lehtinen, B. G. Gustafsson, C. Gustafsson, A.-S. Heiskanen, U. Janas, A. Norkko, C. Slomp, A. Villnäs, M. Voss and M. Zilius (2020) Factors regulating the coastal nutrient filter in the Baltic Sea. *Ambio* **49**, 1194-1210.
50. Thomas, H., J. Pempkowiak, F. Wulff and K. Nagel (2010) The Baltic Sea. In *Carbon and Nutrient Fluxes in Continental Margins: a Global Synthesis*. (Edited by K.-K. Liu, L. Atkinson, R. Q. ones and L. Talaue-McManus), pp. 1-741. Springer.
51. Rolff, C. and R. Elmgren (2000) Use of riverine organic matter in plankton food webs of the Baltic Sea. *Marine Ecology Progress Series* **197**, 81-101.
52. Kullenberg, G. (1981) Chapter 3 Physical Oceanography. In *Elsevier Oceanography Series*, Vol. 30. (Edited by A. Voipio), pp. 135-181. Elsevier.
53. Powers, L. C., J. A. Brandes, A. Stubbins and W. L. Miller (2017) MoDIE: Moderate dissolved inorganic carbon ((DIC)-C-13) isotope enrichment for improved evaluation of DIC photochemical production in natural waters. *Mar. Chem.* **194**, 1-9.
54. Powers, L. C., J. A. Brandes, W. L. Miller and A. Stubbins (2017) Using liquid chromatography-isotope ratio mass spectrometry to measure the delta C-13 of dissolved inorganic carbon photochemically produced from dissolved organic carbon. *Limnol. Oceanogr. Meth.* **15**, 103-115.
55. Powers, L. C. and W. L. Miller (2015) Photochemical production of CO and CO₂ in the Northern Gulf of Mexico: Estimates and challenges for quantifying the impact of photochemistry on carbon cycles. *Mar. Chem.* **171**, 21-35.

56. Koistinen, J., M. Sjöblom and K. Spilling (2020) Determining Inorganic and Organic Carbon. In *Biofuels from Algae: Methods and Protocols*. (Edited by K. Spilling), pp. 63-70. Springer New York, New York, NY.
57. Cauwet, G. (1999) Determination of dissolved organic carbon and nitrogen by high temperature combustion. In *Methods of Seawater Analysis*. (Edited by K. Grasshoff, K. Kremling and M. Ehrhardt), pp. 407-420. Wiley-VCH, Weinheim.
58. Stubbins, A., C. S. Law, G. Uher and R. C. Upstill-Goddard (2011) Carbon monoxide apparent quantum yields and photoproduction in the Tyne estuary. *Biogeosciences* **8**, 703-713.
59. Hu, C. M., F. E. Muller-Karger and R. G. Zepp (2002) Absorbance, absorption coefficient, and apparent quantum yield: A comment on common ambiguity in the use of these optical concepts. *Limnology and Oceanography* **47**, 1261-1267.
60. Hu, C., F. E. Muller-Karger and R. G. Zepp (2002) Absorbance, absorption coefficient, and apparent quantum yield: A comment on common ambiguity in the use of these optical concepts. *Limnology and Oceanography* **47**, 1261-1267.
61. Fichot, C. G. and W. L. Miller (2010) An approach to quantify depth-resolved marine photochemical fluxes using remote sensing: Application to carbon monoxide (CO) photoproduction. *Remote Sens. Environ.* **114**, 1363-1377.
62. Kowalczyk, P., J. Olszewski, M. Darecki and S. Kaczmarek (2005) Empirical relationships between coloured dissolved organic matter (CDOM) absorption and apparent optical properties in Baltic Sea waters. *Int. J. Remote Sens.* **26**, 345-370.
63. Ruggaber, A., R. Dlugi and T. Nakajima (1994) MODELING RADIATION QUANTITIES AND PHOTOLYSIS FREQUENCIES IN THE TROPOSPHERE. *Journal of Atmospheric Chemistry* **18**, 171-210.
64. Koehler, B., T. Landelius, G. A. Weyhenmeyer, N. Machida and L. J. Tranvik (2014) Sunlight-induced carbon dioxide emissions from inland waters. *Glob. Biogeochem. Cycle* **28**, 696-711.
65. Helms, J. R., A. Stubbins, J. D. Ritchie, E. C. Minor, D. J. Kieber and K. Mopper (2008) Absorption spectral slopes and slope ratios as indicators of molecular weight, source, and photobleaching of chromophoric dissolved organic matter. *Limnology and Oceanography* **53**, 955-969.

66. Weishaar, J. L., G. R. Aiken, B. A. Bergamaschi, M. S. Fram, R. Fujii and K. Mopper (2003) Evaluation of specific ultraviolet absorbance as an indicator of the chemical composition and reactivity of dissolved organic carbon. *Environmental Science & Technology* **37**, 4702-4708.
67. Brandes, J. A. (2009) Rapid and precise delta C-13 measurement of dissolved inorganic carbon in natural waters using liquid chromatography coupled to an isotope-ratio mass spectrometer. *Limnol. Oceanogr. Meth.* **7**, 730-739.
68. RCoreTeam (2021) R: A language and environment for statistical computing. The R Foundation for Statistical Computing, Vienna, Austria.
69. Scharnweber, K., S. Peura, K. Attermeyer, S. Bertilsson, L. Bolender, M. Buck, K. Einarsdóttir, S. L. Garcia, R. Gollnisch, C. Grasset, M. Groeneveld, J. A. Hawkes, E. S. Lindström, C. Manthey, R. Övergaard, K. Rengefors, V. T. Sedano-Núñez, L. J. Tranvik and A. J. Székely (2021) Comprehensive analysis of chemical and biological problems associated with browning agents used in aquatic studies. *bioRxiv*, 2021.2002.2026.433092.
70. Jones, R. I. (1992) THE INFLUENCE OF HUMIC SUBSTANCES ON LACUSTRINE PLANKTONIC FOOD-CHAINS. *Hydrobiologia* **229**, 73-91.
71. Lu, C. J., R. Benner, C. G. Fichot, H. Fukuda, Y. Yamashita and H. Ogawa (2016) Sources and Transformations of Dissolved Lignin Phenols and Chromophoric Dissolved Organic Matter in Otsuchi Bay, Japan. *Front. Mar. Sci.* **3**.
72. Sankar, M. S., P. Dash, S. Singh, Y. H. Lu, A. E. Mercer and S. Chen (2019) Effect of photo-biodegradation and biodegradation on the biogeochemical cycling of dissolved organic matter across diverse surface water bodies. *J. Environ. Sci.* **77**, 130-147.
73. Benner, R. and K. Kaiser (2011) Biological and photochemical transformations of amino acids and lignin phenols in riverine dissolved organic matter. *Biogeochemistry* **102**, 209-222.
74. Yang, L., J. Zhang and G. P. Yang (2021) Mixing behavior, biological and photolytic degradation of dissolved organic matter in the East China Sea and the Yellow Sea. *Sci. Total Environ.* **762**, 19.
75. Vione, D. (2016) Photochemical Reactions in Sunlit Surface Waters. In *Applied Photochemistry-When Light Meets Molecules*, Vol. 92. (Edited by G. Bergamini and S. Silvi), pp. 343-376.

76. Minor, E. C., J. Pothen, B. J. Dalzell, H. Abdulla and K. Mopper (2006) Effects of salinity changes on the photodegradation and ultraviolet-visible absorbance of terrestrial dissolved organic matter. *Limnology and Oceanography* **51**, 2181-2186.
77. Seidel, M., M. Manecki, D. P. R. Herlemann, B. Deutsch, D. Schulz-Bull, K. Jürgens and T. Dittmar (2017) Composition and Transformation of Dissolved Organic Matter in the Baltic Sea. *Front. Earth Sci.* **5**.
78. Bauer, J. E. and T. S. Bianchi (2011) Dissolved Organic Carbon Cycling and Transformation. In *Treatise on Estuarine and Coastal Science, Vol 5: Biogeochemistry*. (Edited by E. Wolanski and D. McLusky), pp. 7-67. Elsevier Academic Press Inc, San Diego.
79. Nelson, N. B., C. A. Carlson and D. K. Steinberg (2004) Production of chromophoric dissolved organic matter by Sargasso Sea microbes. *Mar. Chem.* **89**, 273-287.
80. Stubbins, A., R. Spencer, H. Chen, P. Hatcher, K. Mopper, P. Hernes, V. Mwamba, A. Mangangu, J. Wabakanghanzi and J. Six (2010) Illuminated darkness: Molecular signatures of Congo River dissolved organic matter and its photochemical alteration as revealed by ultrahigh precision mass spectrometry. *Limnology and Oceanography* **55**, 1467-1477.
81. Obernosterer, I. and R. Benner (2004) Competition between biological and photochemical processes in the mineralization of dissolved organic carbon. *Limnology and Oceanography* **49**, 117-124.
82. Johannessen, S. C., M. A. Pena and M. L. Quenneville (2007) Photochemical production of carbon dioxide during a coastal phytoplankton bloom. *Estuar. Coast. Shelf Sci.* **73**, 236-242.
83. Bittar, T. B., A. A. H. Vieira, A. Stubbins and K. Mopper (2015) Competition between photochemical and biological degradation of dissolved organic matter from the cyanobacteria *Microcystis aeruginosa*. *Limnology and Oceanography* **60**, 1172-1194.
84. Helms, J. R., J. Mao, A. Stubbins, K. Schmidt-Rohr, R. G. M. Spencer, P. J. Hernes and K. Mopper (2014) Loss of optical and molecular indicators of terrigenous dissolved organic matter during long-term photobleaching. *Aquatic Sciences* **76**, 353-373.
85. Budac, D. and P. Wan (1992) PHOTODECARBOXYLATION - MECHANISM AND SYNTHETIC UTILITY. *J. Photochem. Photobiol. A-Chem.* **67**, 135-166.

86. Bertilsson, S. and L. J. Tranvik (1998) Photochemically produced carboxylic acids as substrates for freshwater bacterioplankton. *Limnology and Oceanography* **43**, 885-895.
87. Mopper, K. and D. J. Kieber (2002) Chapter 9 - Photochemistry and the Cycling of Carbon, Sulfur, Nitrogen and Phosphorus. *Biogeochemistry of Marine Dissolved Organic Matter*, 455-507.

FIGURE CAPTIONS

Figure 1. Ratios of chromophoric dissolved organic matter absorption coefficient a), c), e) versus photon doses ($Q_a(int)$, mol photons absorbed), and b), d), f) versus time (day), for JOMEX amendment experiment samples that reflect the *in situ* conditions, a) b) at 280 nm, $a_g(280)_T : a_g(280)_{T0}$; c) d) at 400 nm, $a_g(400)_T : a_g(400)_{T0}$; e) f) integrated from 280 nm to 400 nm, $a_g(int)_T : a_g(int)_{T0}$. Ratios were calculated as values at different days to those at experimental day 1 (immediately after amendment).

Figure 2. Chromophoric dissolved organic matter absorption coefficients (a_g , m^{-1}) versus wavelength λ (nm) of mesocosm samples on experimental days 1, 3, 6, 8, 10, and 13 of the JOMEX experiment. Day 1 was the day of initial amendment and corresponds to the darkest color in each treatment, the color became lighter over time, and day 13 corresponds to the lightest color.

Figure 3. Ratios of chromophoric dissolved organic matter absorption coefficients at a) d) g) 280 nm ($a_g(280)_T : a_g(280)_{T0}$), b) e) h) 400 nm ($a_g(400)_T : a_g(400)_{T0}$), and c) f) i) integrated over 280-400 nm ($a_g(int)_T : a_g(int)_{T0}$) versus photon dose ($Q_a(int)$, mmol photons absorbed) for laboratory irradiation experiments conducted on mesocosm samples of the JOMEX experiment (day 1 was the day of initial amendment). Ratios were calculated by dividing the corresponding a_g at time T by that at time T_0 .

Figure 4. a) Chromophoric dissolved organic matter absorption spectral slope $S_{275-295}$ (nm^{-1}) versus photon doses ($Q_a(int)$, mol photons absorbed) for JOMEX amendment experiment samples that reflect the *in situ* conditions; b) $S_{275-295}$ versus time (experimental day, day 1 was the day of initial amendment). Error bars were ± 1 standard error for $S_{275-295}$ (linear regression slopes of natural-log-transformed absorbance versus wavelength at 275-295 nm).

Figure 5. Chromophoric dissolved organic matter absorption spectral slope $S_{275-295}$ (nm^{-1}) versus photon dose ($Q_a(int)$, mmol photons absorbed) for individual laboratory experiments, using mesocosm samples of the JOMEX amendment experiment. Error bars were ± 1 standard error for $S_{275-295}$ (linear regression slopes of natural-log-transformed absorbance versus wavelength at 275-295 nm).

Figure 6. Dissolved organic carbon (DOC) concentrations (mg L^{-1}) a) versus photon dose ($Q_a(int)$, mol photons absorbed), and b) versus time (day), for JOMEX amendment experiment samples that reflect the *in situ* conditions. Day 1 was the day of initial amendment.

Figure 7. Specific ultraviolet absorbance $SUVA_{254}$ ($\text{L mg}^{-1} \text{m}^{-1}$) a) versus photon doses ($Q_a(int)$, mol photons absorbed), and b) versus time (day), for JOMEX amendment experiment samples that reflect the *in situ* conditions. Day 1 was the day of initial amendment. c-f) $SUVA_{254}$ versus photon dose ($Q_a(int)$, mmol photons absorbed) for laboratory irradiation experiments using mesocosm samples of the JOMEX amendment experiment.

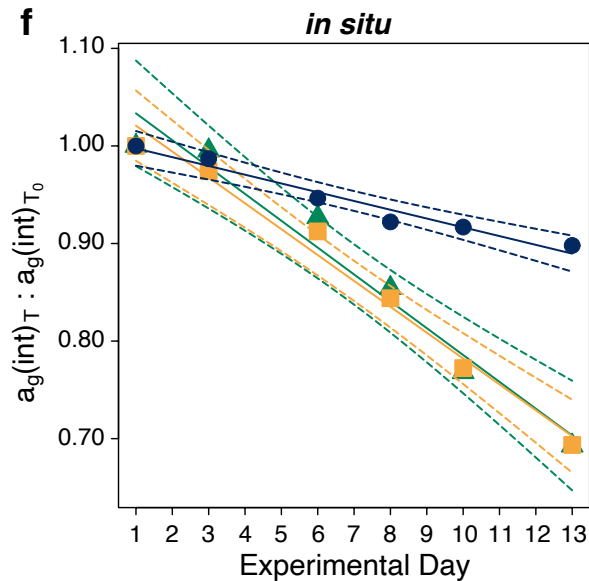
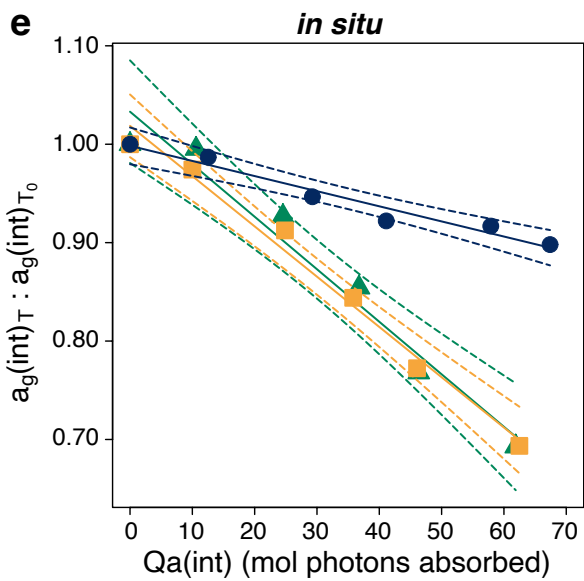
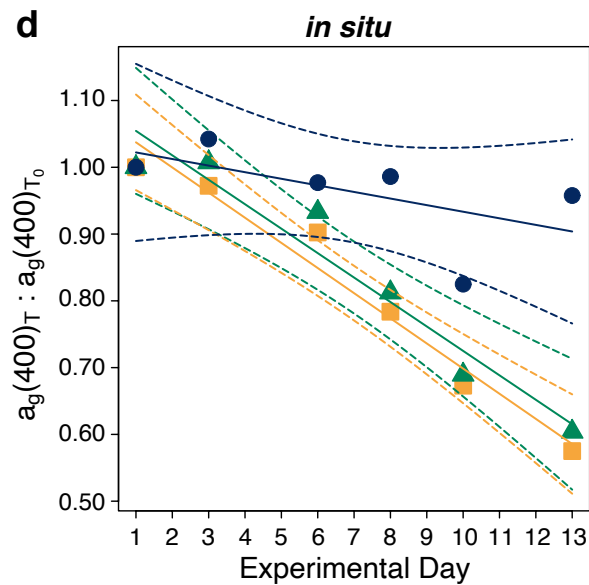
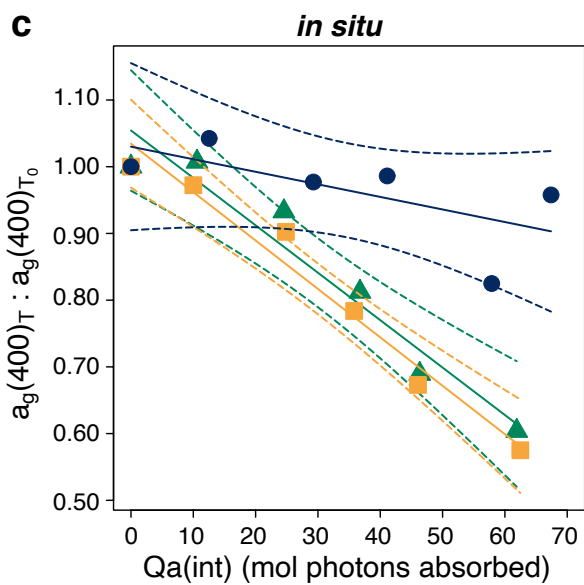
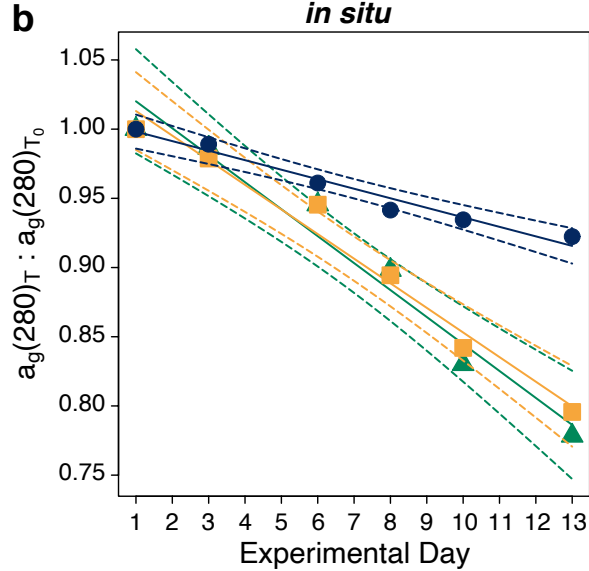
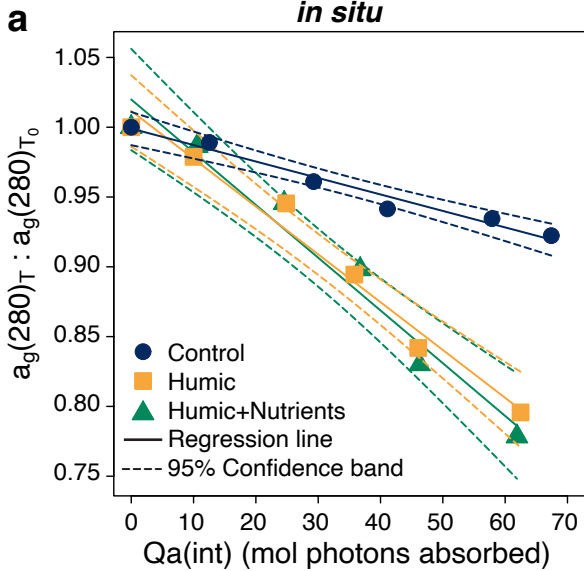
Figure 8. Dissolved inorganic carbon (DIC) photoproduction rates (P_{DIC} , μM (mmol photon absorbed) $^{-1}$) for laboratory irradiation experiments using mesocosm samples from JOMEX amendment experiment. Day 1 was the day of initial amendment. Rates were slopes of linear regressions of photochemically produced DIC concentrations (DIC_{photo} , μM) versus photon absorbed by CDOM (mmol photons absorbed), error bars were ± 1 standard error of the slope.

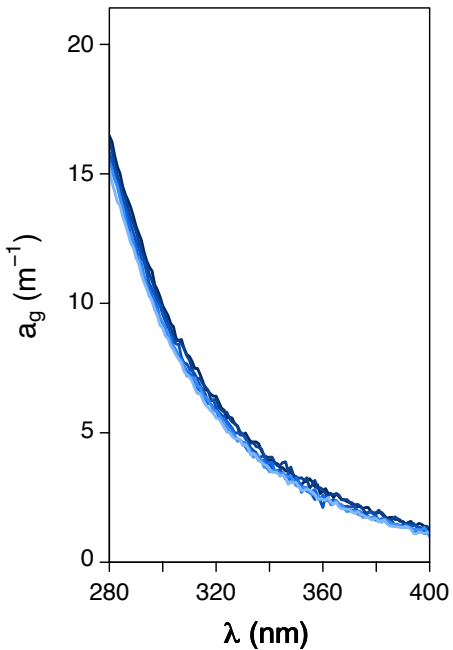
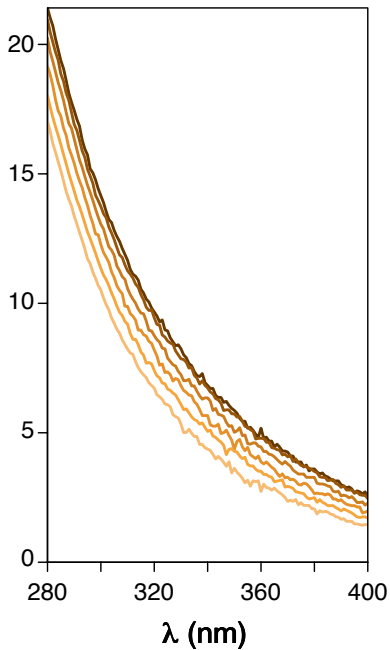
Table 1. Initial chromophoric dissolved organic matter absorption coefficients at 280 nm, 400 nm, and integrated over 280 - 400 nm ($a_g(280)$ (m^{-1}), $a_g(400)$ (m^{-1}), and $a_g(int)$ ($\text{m}^{-1} \text{ nm}$), respectively), dissolved organic carbon concentrations ([DOC], mg L^{-1}) and specific ultraviolet absorbance at 254 nm ($SUVA_{254}$, $\text{L mg}^{-1} \text{ m}^{-1}$), for JOMEX amendment experiment. These initial values reflect the *in situ* conditions in the JOMEX mesocosms and starting conditions for laboratory irradiation experiments. Days represent experimental days, and day 1 was the day of initial amendment. Irradiation time (h) were irradiation time points for laboratory irradiation experiments using samples from different days of the JOMEX experiment.

Day	Irradiation time (h)	Control					Humic					Humic+Nutrients				
		$a_g(280)$ (m^{-1})	$a_g(400)$ (m^{-1})	$a_g(int)$ ($\text{m}^{-1} \text{ nm}$)	[DOC] (mg L^{-1})	$SUVA_{254}$ ($\text{L mg}^{-1} \text{ m}^{-1}$)	$a_g(280)$ (m^{-1})	$a_g(400)$ (m^{-1})	$a_g(int)$ ($\text{m}^{-1} \text{ nm}$)	[DOC] (mg L^{-1})	$SUVA_{254}$ ($\text{L mg}^{-1} \text{ m}^{-1}$)	$a_g(280)$ (m^{-1})	$a_g(400)$ (m^{-1})	$a_g(int)$ ($\text{m}^{-1} \text{ nm}$)	[DOC] (mg L^{-1})	$SUVA_{254}$ ($\text{L mg}^{-1} \text{ m}^{-1}$)
1	0, 2, 5, 12, 19, 27	16.5	1.19	666	5.2	2.1	21.4	2.53	988	5.5	2.4	21.3	2.43	993	6.3	2.1
3	0, 4, 8, 14, 24, 36	16.3	1.24	657	5.2	2.1	21.0	2.46	984	5.4	2.5	21.0	2.44	989	5.1	2.6
6	0, 4, 8, 14, 24, 36	15.8	1.17	630	5.0	2.1	20.2	2.28	922	5.4	2.4	20.1	2.26	921	5.2	2.5
8	0, 4, 8, 14.1, 24.1, 36.1	15.5	1.18	614	4.8	2.2	19.1	1.98	853	5.1	2.4	19.1	1.97	849	5.2	2.4
10	0, 4, 8, 14, 24, 36	15.4	0.98	611	4.9	2.1	18.0	1.70	780	5.1	2.3	17.7	1.67	763	6.8	1.7
13	0, 4, 8, 14, 24, 36	15.2	1.14	598	4.8	2.1	17.0	1.45	701	5.1	2.2	16.6	1.46	688	5.0	2.2

Table 2. Chromophoric dissolved organic matter (CDOM) absorption coefficient a_g fading rates (mean \pm 1SE), at 280 nm ($a_g(280)$), 400 nm ($a_g(400)$) (m^{-1} (mol photons absorbed) $^{-1}$), and for integrated a_g over 280-400 nm ($a_g(int)$) (m^{-1} nm (mol photons absorbed) $^{-1}$), *in situ*, in laboratory irradiation experiments of the JOMEX experiment mesocosm samples from different days (day 1 was the day of initial amendment), and in laboratory irradiation experiment of HuminFeed in Milli-Q ultrapure water (2 mg L $^{-1}$ concentration). Laboratory a_g fading rates were calculated by linear regressions of a_g versus photons absorbed by CDOM in the samples, and *in situ* rates were calculated by linear regressions of a_g versus estimated *in situ* photon dose. All rates were statistically significant (linear regressions, $p < 0.05$) except for the ones in grey.

Treatment	<i>in situ</i>	Laboratory irradiation experiments of mesocosm samples						HuminFeed® in water
		Day 1	Day 3	Day 6	Day 8	Day 10	Day 13	
$a_g(280)$: absorption at 280 nm								(m^{-1} (mol photons absorbed) $^{-1}$)
Control	-0.019430 \pm 0.0016770	-2043.9 \pm 120.87	-1104.8 \pm 76.694	-1379.1 \pm 78.087	-1227.8 \pm 68.923	-1287.8 \pm 40.721	-1336.4 \pm 122.57	-
Humic	-0.073339 \pm 0.0053850	-985.05 \pm 80.298	-729.84 \pm 114.22	-1046.2 \pm 77.801	-1238.4 \pm 127.95	-812.01 \pm 123.13	-1188.2 \pm 120.45	-445.58 \pm 52.317
Humic+Nutrients	-0.080494 \pm 0.0076050	-838.88 \pm 63.283	-865.54 \pm 72.941	-948.28 \pm 114.14	-1019.8 \pm 90.589	-1035.1 \pm 95.695	-1398.0 \pm 78.972	-
$a_g(400)$: absorption at 400 nm								(m^{-1} (mol photons absorbed) $^{-1}$)
Control	-0.0022460 \pm 0.0012810	-174.44 \pm 76.034	-40.906 \pm 52.144	-128.53 \pm 14.565	-147.71 \pm 41.648	-43.833 \pm 73.144	-98.114 \pm 26.411	-
Humic	-0.018342 \pm 0.0016410	-202.85 \pm 24.095	-63.226 \pm 30.507	-162.72 \pm 24.192	-172.54 \pm 39.923	-114.65 \pm 48.516	-98.671 \pm 35.571	-188.80 \pm 37.097
Humic+Nutrients	-0.017235 \pm 0.0021540	-99.303 \pm 41.843	-167.42 \pm 14.965	-164.52 \pm 32.958	-157.46 \pm 34.400	-213.57 \pm 41.808	-195.82 \pm 40.010	-
$a_g(int)$: absorption integrated over 280-400 nm								(m^{-1} nm (mol photons absorbed) $^{-1}$)
Control	-1.0232 \pm 0.10660	-97988 \pm 10492	-44696 \pm 3653.7	-57853 \pm 3466.5	-50450 \pm 1415.5	-49018 \pm 4872.6	-50724 \pm 2889.0	-
Humic	-5.1619 \pm 0.31680	-57712 \pm 5447.4	-44557 \pm 6121.7	-57659 \pm 3971.0	-64258 \pm 8544.6	-36571 \pm 10301	-42085 \pm 8188.1	-41557 \pm 5461.3
Humic+Nutrients	-5.3015 \pm 0.50950	-43482 \pm 5216.5	-47918 \pm 3211.3	-55002 \pm 3871.3	-54307 \pm 3504.7	-53626 \pm 5244.9	-71232 \pm 3267.2	-



Control**Humic****Humic + Nutrients**